PAPERS IN PHYSICAL OCEANOGRAPHY AND METEOROLOGY

PUBLISHED BY

MASSACHUSETTS INSTITUTE OF TECHNOLOGY

AND

WOODS HOLE OCEANOGRAPHIC INSTITUTION

VOL. XIII, NO. 2

ON THE STRUCTURE OF THE TRADE WIND MOIST LAYER

BY

JOANNE STARR MALKUS

Contribution No. 969 from the Woods Hole Oceanographic Institution

---

CAMBRIDGE AND WOODS HOLE, MASSACHUSETTS

AUGUST, 1958

CONTENTS

INTRODUCTION

The Trade-Wind Region and Its Role in Global Meteorology

The trade-wind zone extends from about 10 to 25 degrees latitude on either side of the thermal equator. Steady easterlies, with an equatorward component, dominate the surface of the globe in both hemispheres, from the subtropical ridge line all the way to the equatorial trough.

In the vertical, trade-wind air is characterized by its layered structure, illustrated schematically in Figure 1. A lower moist convective layer commonly extends to a height of about 2 kilometers, topped by a much drier layer aloft. The transition zone, a few hundred meters in thickness, is called the "trade-wind inversion". A region of rapid drying and usually of stabilization in temperature lapse rate, its mean level is determined by the balance of the opposing effects of subsidence and convection. It gradually weakens and rises in height downstream as convection spreads moisture upward against the diminishing brake of subsidence, which decreases as the air leaves the influence of the subtropical high-pressure cell.

The trade-wind moist layer forms an early link in the chain of the atmospheric energy supply. This begins with the tropical oceans. Largely in latent form of water vapor, the energy first enters the lowest air at the roughened sea boundary in a manner which ultimately must be controlled by molecular processes. It is then spread vertically and shipped equatorward, with increasingly large scales of motion playing a role in its transport.

First the vapor is stirred upward through a well-mixed surface layer by thermal-turbulent eddies 50–150 meters in diameter. At about 650 meters or 2,000 feet, the water vapor condensation level is reached and some of the wetter eddies condense to form clusters of small cloudlets. Small clouds aggregate into larger trade cumuli (typical photograph in Figure 2) which, fighting against entrainment or dilution by mixing, distribute water vapor through a several kilometer deep moist layer, but only a few are able to shoot towers into the dry air above the inversion.

As the trade-wind air flows westward and equatorward, myriads of these cumuli, growing in bunches day and night, build up the moist layer and load the lower air with latent heat. By overshooting towers, they gradually raise and weaken the inversion, which becomes less and less frequently observed in the downstream portions of the trades. There the previously steady current, stable to perturbations in its inversion-dominated poleward half, becomes unstable and breaks down into wave-like and vortical disturbances which in the equatorial trough zone are the rule and not the exception. In these, the cumuli grow to enormous cumulonimbus, funnelling surface air up to the tropopause. The consequent release of the accumulated latent heat balances local radiation loss and, on the average, leaves enough over to be exported aloft to middle latitudes, overcoming the deficits and maintaining the circulations there. The amount of latent heat available for release in the equatorial trough and thus for supply aloft to the westerlies across the subtropical ridge depends initially upon the accumulation by the lower trade, which in turn depends upon the efficacy of small-scale turbulent and convective process at the air-sea boundary.

The average structure of the inversion-dominated portion of the trade has received serious study in the past ten years (17). Treated as a quasi-steady circulation, the major features of its dynamics and energy budget have been outlined (10, 18). It has been shown to be a self-maintaining, energy exporting circulation branch, about 75–80% of the export being in the form of the latent heat mentioned above and the remainder in sensible heat form. The latter, largely derived from internal conversion of latent to sensible heat by convective precipitation, is small but vital; it produces the downstream pressure drop maintaining the flow against friction and providing the slight excess for downstream divergence.

A crude theoretical study of fluctuations in the outer trade was made in (10) in the latter context. The proportionality in a two-dimensional current (as this portion of the system seems to be) between subsidence and downstream divergence suggested a stable "feedback" between the convective scale of motion and the overall flow. Since subsidence is a major brake on convection, if convective warming became greater than normal, enhanced subsidence would begin to suppress it, and if convection died out, reduced

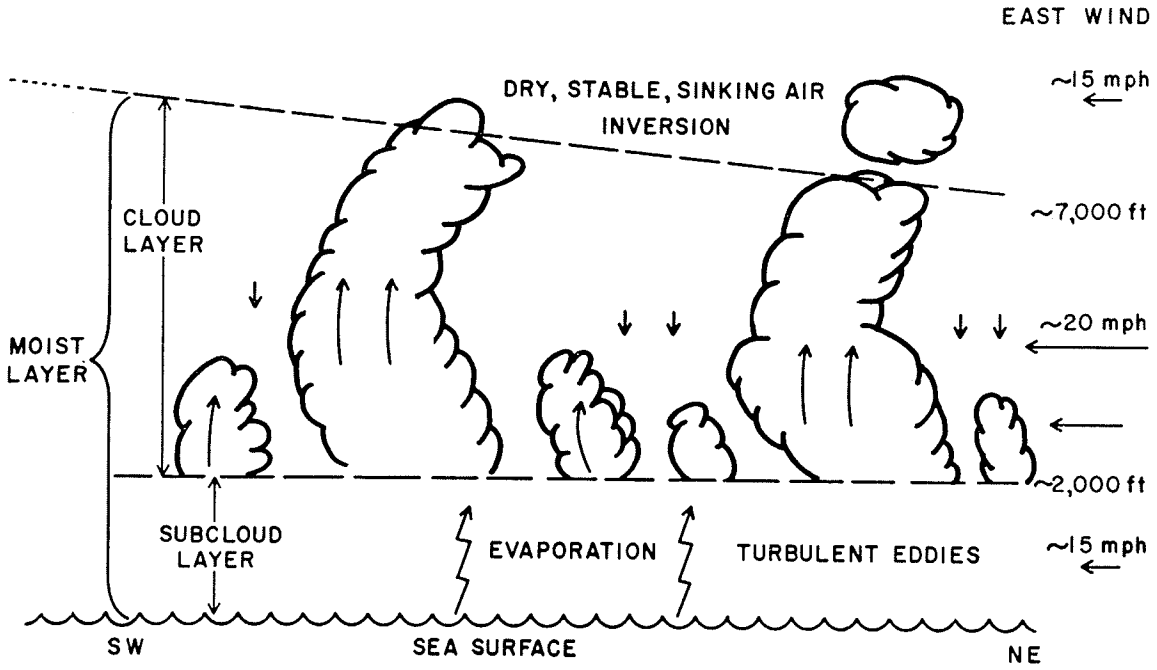

FIGURE 1. Schematic vertical cross section along the path of the trade winds. Typical wind speeds at the various levels are indicated by arrows at the right. The moist layer deepens by about 1,000 feet in 500 miles horizontal distance; clouds are thus drawn much larger than to actual scale.

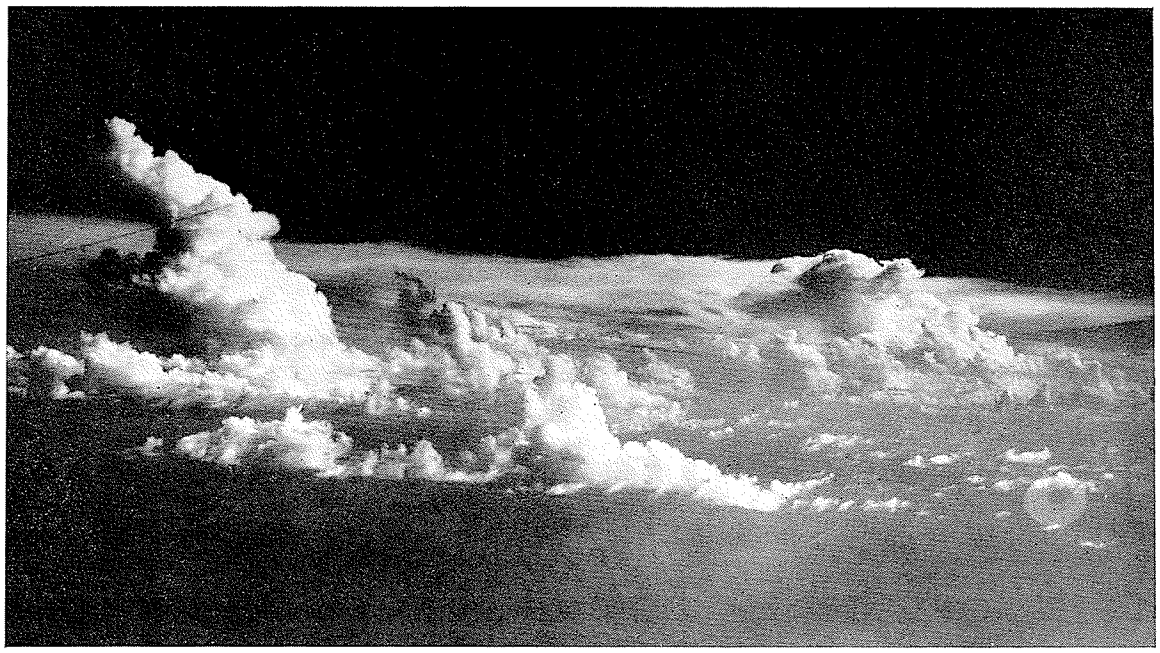

FIGURE 2. Typical aerial photograph of a trade cumulus group over the ocean near Puerto Rico, showing small cloudlets, larger towers with pronounced backslant (wind blows from left) and thin stratus sheet formed by cumulus spreading just below inversion base.

warming and consequently reduced subsidence would permit it to be restored. That the marked steadiness of the flow is confined to the convective layer supports this suggestion and turns our attention to variations in moist layer convection and its interaction with the larger-scale structure of the trade.

Alterations in its latent heat export are of particular significance since this constitutes the energy supply for large-scale circulations ranging from tropical storms to zonal westerlies. It is conceivable that fluctuations in these latter may be partially forced or triggered by variations in the energy source. And although the trades vary relatively little compared to other wind systems, the possibility that their small variations lead to large differences in local or even integrated moisture export is a real one, since their average speed of 6–7 m/sec is close to the critical wind speed for ocean whitecap formation. Riehl (16) cites evidence that the evaporation rate from the sea surface may increase sharply when whitecaps and spray appear, and has therefore suggested a correlation between tropical index cycle and that of the westerlies.

We propose here to tackle the tropical phase of the problem by inquiring from observations how the convective structure of the moist layer varies between conditions of weak and strong trade. After having described these variations, we further ask what might be the mechanisms producing them, and how they might affect the role of the trades in global circulations. Fortunately, suitable data are now available from one location and season in the western Atlantic in such widely different phases of the index cycle that a maximum contrast should be possible.

The Data and Method of Observation

Two sets of aircraft temperature and moisture soundings were obtained over the oceans near Puerto Rico (lat. 19°N; long. 66°W) in the spring season of different years. The first series was made during April 1946 by the Wyman-Woodcock expedition and later analyzed by Bunker, Haurwitz, Malkus, and Stommel (4). During this period the trades were strong from the northeast and trade cumulus convection was vigorous. Disturbances were few and relatively weak.

Seven years later, in March–April 1953, the Woods Hole group again visited the region, in collaboration with the Department of Meteorology of the Imperial College, London, and the British National Institute of Oceanography. This time the trades were subnormal and were veered around to south of east for most of the period. Ordinary trade cumulus convection was feeble, although several intense disturbances accompanied by large cumulonimbus build-ups passed through.

The instrumentation and method of obtaining the soundings were nearly identical in the two series. A revised version of the M.I.T. psychrograph was mounted on a PBY aircraft. Dry and wet-bulb temperatures were recorded as the plane spiralled upward at about 200 ft/min, a slow enough rate of climb for lag free readings to be obtained. The spirals were about two miles in diameter and in the 1953 series they were frequently made around smoke flares which had been dropped to determine the surface wind direction. Vertical wind structure was obtained from the British group which made double theodolite pilot balloon observations from Anegada Island (18° 50′N; 64°20′W) 120 miles east-northeast of San Juan (where the aircraft was based) and generally within twenty miles of the observing area. The 1946 spirals were in the vicinity of a small research vessel which supplied surface wind information.

For the 1953 series a wide-angle, time-lapse motion picture camera was used from the nose of the aircraft during all soundings. This made it possible to determine the location of the spirals relative to cloud groups and to assess the state of the sea surface. For the 1946 data this was done from the notes of the aircraft and ship observers.

The accuracy of the observations and the method of reduction has been described in detail in (4), in which the 1946 sounding data are tabulated. The 1953 soundings appear in Appendix I of this paper, where temperature, mixing ratio, virtual and potential temperature are given as functions of true altitude and pressure.

The Synoptic Situation in the Western Atlantic during the 1946 and 1953 Observing Periods

The period of April 10–28, 1946, was one of relatively strong undisturbed trade. The average (shipboard) wind speed for all observing days was 9.1 m/sec and the sea was generally rough with whitecaps present. The trajectories of the air reaching the observing region were from north of

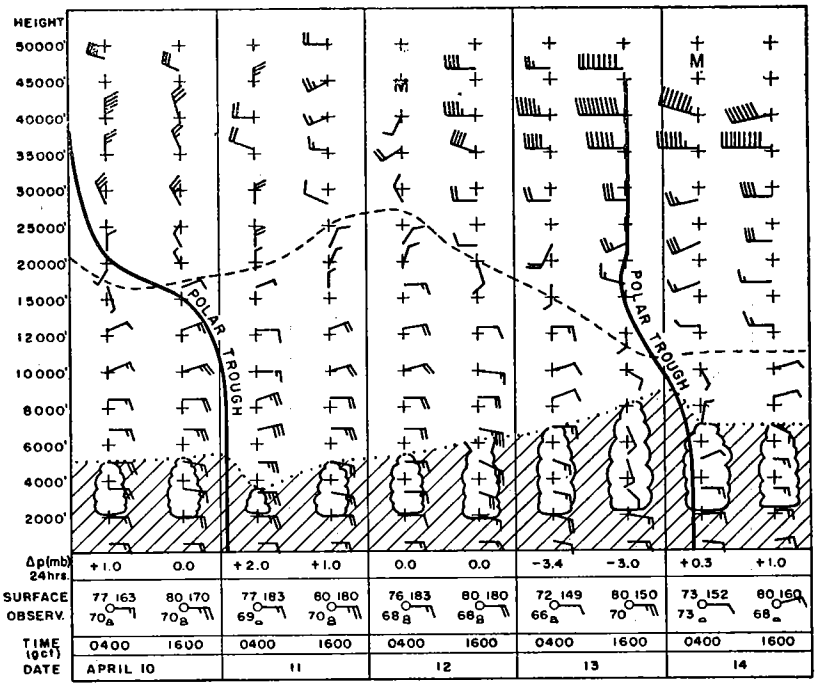

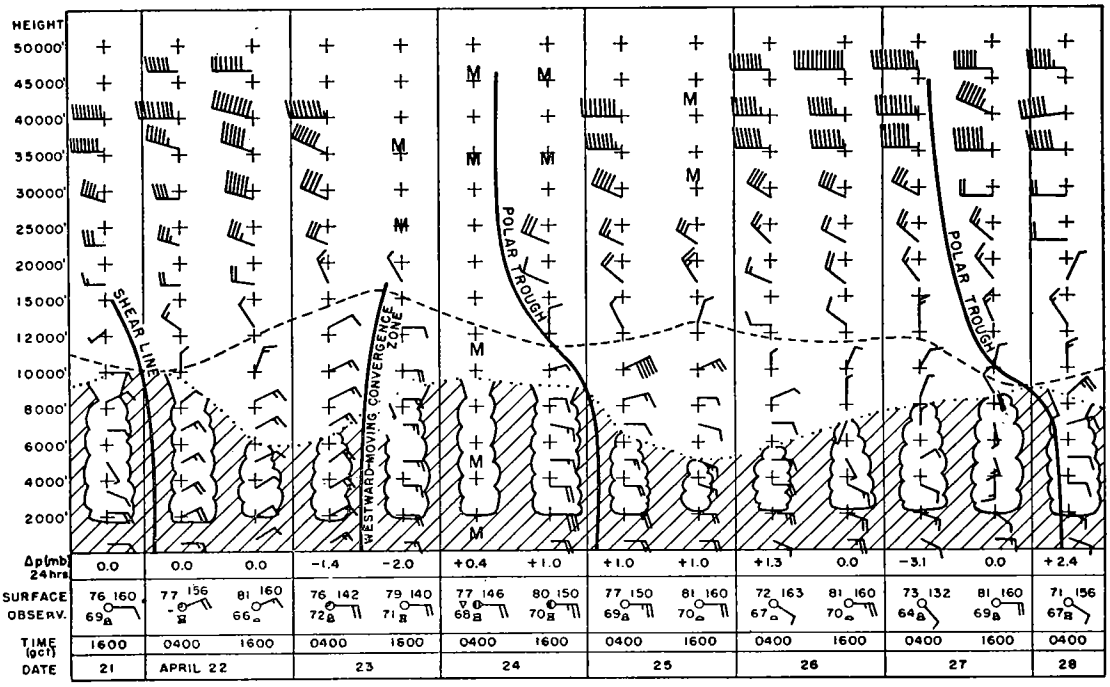

3A

FIGURE 3. Time cross sections for the two observing periods April 10–28, 1946 (H), Figure 3A, and March 18–April 7, 1953 (L), Figure 3B covering observation days only. Upper winds are radio winds. A short barb indicates a speed of 5 miles per hour, a long barb 10 miles per hour. Surface winds are in Beaufort scale. The hatched region is the moist layer, the top of which is represented by a dotted line. The base of the westerlies is indicated by a dashed line. The greater strength of disturbances in the L period is suggested by more middle and upper cloudiness.

east. The subtropical high-pressure cell was well developed, elongated from east to west, and maintained a central pressure departing little from 1023 mb. Rather little low-level flow across it occurred during the period. The time cross section for all observing days and a typical surface map are shown in Figures 3A and 4A.

The period of March 18–April 7, 1953 was one of weaker, more disturbed trade regime. The surface winds in the observing area averaged 5.7 m/sec and no whitecaps were seen on seven of the nine days. The time cross section is shown in Figure 3B and a typical surface map in Figure 4B. They show that travelling disturbances were more intense at all levels than in the same period of 1946. Middle and high cloudiness are frequent on the 1953 time section, while none are reported on that of 1946. Relatively lower zonal index

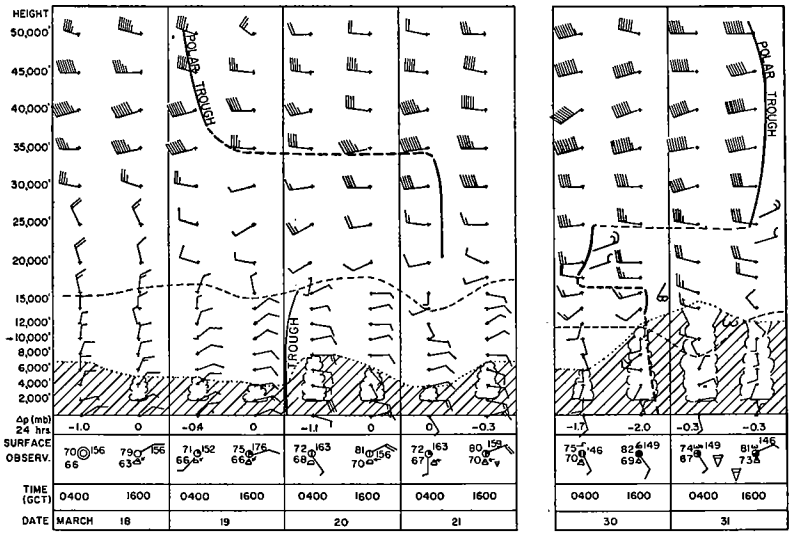

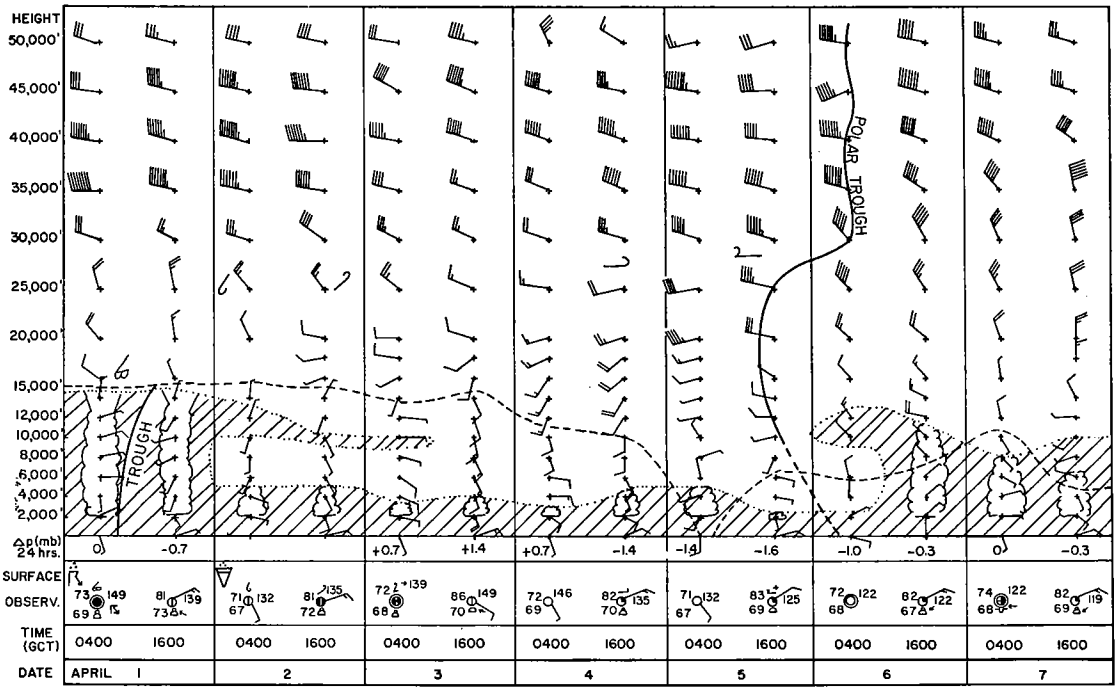

3B

during the 1953 observation period is suggested by Figures 3 and 4 and further by Figure 5. The latter is a plot of the central pressure of the subtropical high cell, which averaged less than 1017 mb on all 1953 observing days and decreased markedly from the beginning to the end of the period. Not only did the zonal (easterly) wind component fall off, but it is likely that the meridional trade-wind cell in the western Atlantic was concomitantly running down. The equatorward component of flow disappears and actually reverses between March 30 and April 5, and the trajectories of the air reaching San Juan are from south of east.

It may thus be considered that the 1946 soundings show air structure typical of strong circulation (for the location and season) and the 1953 soundings show the features of weak circula-

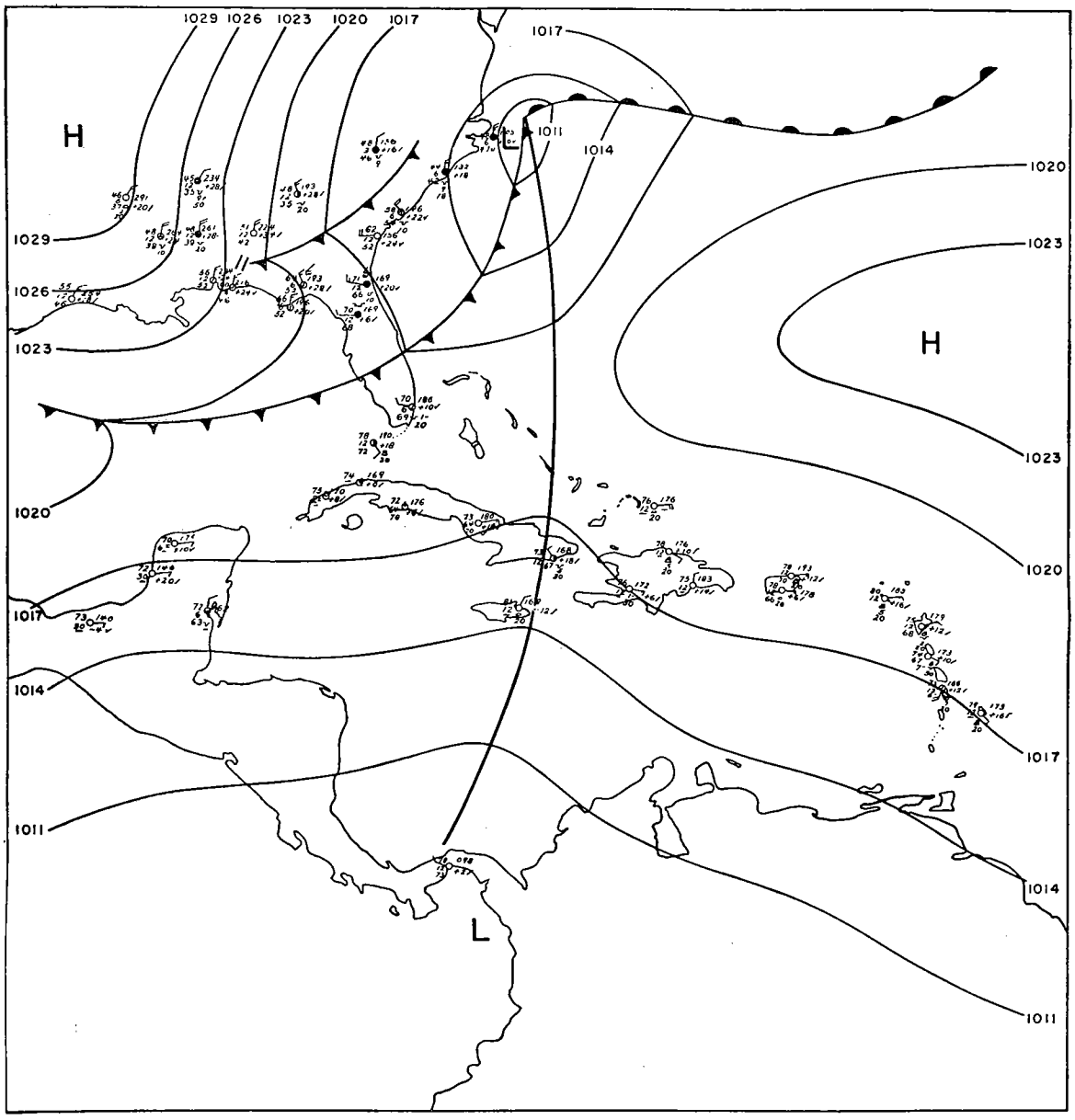

4A

FIGURE 4. Typical surface charts for the two observing periods. In each case the heavy solid line denotes a polar trough. Figure 4A is the chart for April 12, 1946, 1230 GCT, chosen as typical of the H period and Figure 4B is the chart for March 29, 1953, 1830 GCT, chosen as typical of the L period. Note the weaker subtropical high-pressure cell and relative north-south elongation of pressure systems on the latter.

tion at the same place and season. They will therefore be designated as series H and L, respectively, throughout the rest of this report. It is interesting to note further that the mean wind strength in the two series falls clearly on opposite sides of the transition to rough sea and whitecaps, which were always present in series H and nearly always absent in series L.

Outline of the Present Study

The trade-wind moist layer is itself subdivided in the vertical into two superposed layers of different convective regime, because of the occurrence of water vapor condensation at about 600–700 m above the tropical oceans. Below the condensation level, in the so-called "subcloud" layer, unsaturated convective turbulence predominates. Eddies 50–150 m across are characteristic and recent studies (11) suggest that larger scales of motion with dimensions 10–50 km (size of cloud groups) are also significant. No evidence of cloud-scale motions below cloud base have been found, except in precipitating downdrafts. Above the condensation level, cumulus convection is the major transport process; small-scale turbulence is confined to the neighborhood of clouds, which form in bunches separated by wider, weakly subsiding clear areas.

The lower four-fifths of the subcloud layer is well-stirred and has been christened the "mixed layer". The lapse rate is close to dry adiabatic and the moisture content of the air is nearly constant with height, decreasing only 3–6% from 15 m above the sea to its top at about 550 m. The thickness of the mixed layer commonly shows variations of 20% in space and as much as 100% in time, with extreme day-to-day variations of about 300–700 m. Recent evidence suggests that its space variations on a 10–50 km scale are associated with the bunchy grouping of trade cumuli. It appears that the clouds are grouped in places where the mixed layer is thickened, reaching close to the condensation level of the air within it.

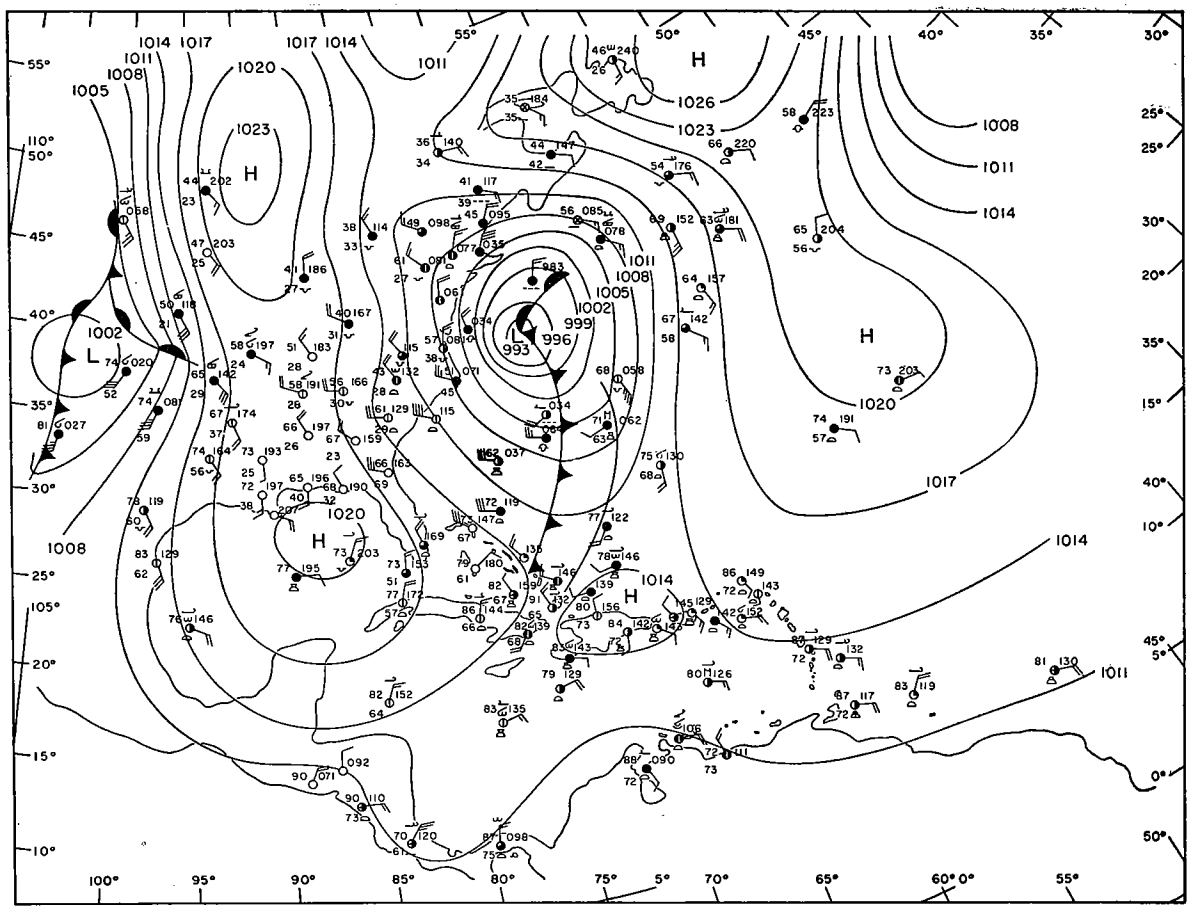

4B

The trade-wind mixed layer thus plays the crucial role of a "valve" in the earliest phases of the atmosphere's energy supply. Its structure regulates both the input from the sea below through evaporation and the output aloft through cumulus formation. The present study has therefore been divided into three parts. Part I examines the structure of air below cloud; Part II is concerned with the features of the cloud layer and cumulus convection; and Part III attempts to construct a physical model of the operation of the moist layer as a whole.

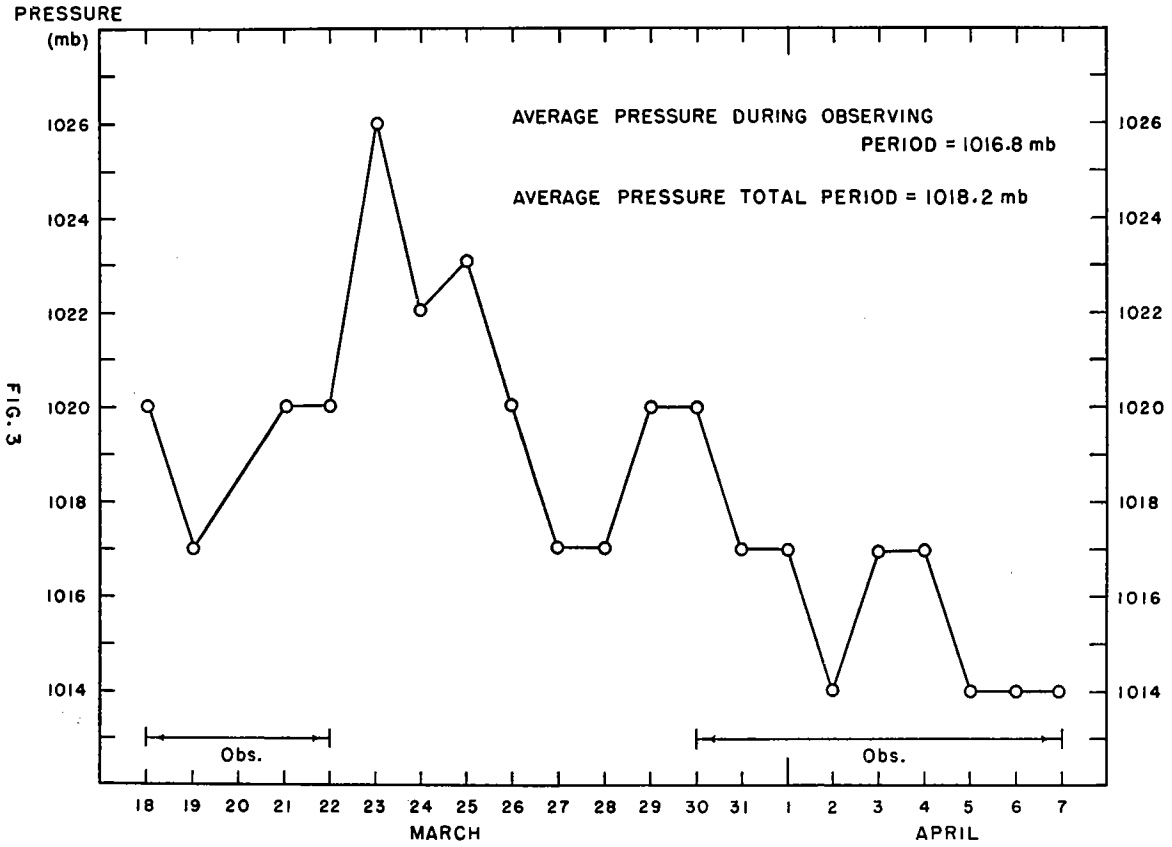

FIG. 3

FIGURE 5. Plot of the central pressure of the subtropical high cell during the 1953 (L) observing period as a function of time as taken from the daily surface chart at 1830 GCT.

PART I

ON THE STRUCTURE OF TRADE-WIND AIR BELOW CLOUD

The Questions Raised

This section concerns the structure of the lowest air and how it varies between conditions of strong and weak trade. Specifically we wish to study the functions and properties of the mixed layer (defined and located on temperature-moisture soundings by its nearly constant mixing ratio and close to adiabatic lapse rate). In the context of the Introduction, some questions of particular interest are:

1. What are the vertical fluxes of sensible and latent heat? According to classical turbulence theories, the former should be nearly always downward in the trades, since potential temperature almost invariably increases with height above the lowest few meters. Recently countergradient heat flows have been hypothesized and confirmed observationally elsewhere in the atmosphere (3). Although the sensible heat accumulation by the lower trade is only about 25% that of the latent, it has been shown (18) essential in the maintenance of the flow. Thus the direction and magnitude of its vertical flux remains an important unresolved question. The water vapor flux, on the other hand, is clearly always upward but, as suggested in the introduction, may vary widely. We wish to inquire how this variation affects and is affected by the structure of the lower trade.
2. Why were trade cumuli both sparse and poorly developed in series L (1953) compared to series H (1946)? Is the difference in cumulus convection attributable to suppression of convective transports in the subcloud layer or must we look for brakes such as abnormal stability or dryness in the cloud layer itself?
3. What is the mechanism of maintenance of convective-turbulence in the mixed layer itself and the relative roles of buoyancy and wind stirring therein? The vertical transports in the lower trades are undoubtedly a combination of turbulent shear flow and thermal turbulence in a fluid heated from below. The relative importance of these and the effect of their interaction has not been assessed.

Comparison of the Data

The series L soundings have been analyzed and compared with those of series H (already analyzed and discussed in (4)) with these questions in mind. Although it is not yet possible to give definite answers to the first and third, nor to make an experiment isolating a single factor alone (such as wind strength or sea surface roughness), the differences in subcloud air structure in the two periods suggests that important fluctuations in energy input and transfer accompany changes in flow regime in this critical source region. The nature and magnitude of these differences give some clues as to their origin and possible effects upon other parts of the atmosphere.

A summary of the major features of the mixed layer for series L is presented in Table 1. A comparison of the H and L series appears in Table 2, subdivided into clear and cloudy area soundings. The right-hand five columns of Table 1 were obtained by calculations from the soundings as follows: Plots of temperature, virtual temperature, and mixing ratio against height were made and the lapse rate of each determined graphically and then checked by the method of least squares. The height, h, of the mixed layer was determined as in (4) for series H, by picking the height at which the mixing ratio lapse rate increased suddenly. This level was usually well defined and was accompanied in most cases by a stabilization in temperature lapse rate. The lifting condensation level, LCL, was found from a tephigram, using the mean properties of the mixed layer.

In series H, the temperature lapse rate in the mixed layer was always slightly subadiabatic. In series L, on the other hand, one case of superadiabatic mixed layer was found, namely, that of the sounding of April 2. This was a day of particularly light wind and the nose camera film showed the calmest sea of the period. On the remaining L days the lapse rate was slightly stable, varying around an average value of 0.9 dry adiabatic, as in series H. The lapse rate of virtual temperature averaged 4% greater than the temperature lapse rate, but in no case went over to superadiabatic when the temperature lapse rate was subadiabatic.

A rough calculation sheds light on the role of buoyancy. In the case of the average lapse rate of virtual temperature, T*, it may be shown that buoyant bubbles leaving the sea surface with

TABLE 1. SUMMARY OF FEATURES OF MIXED LAYER FOR 1953 (SERIES L) SOUNDINGS.

Date	Time	Location	Local Wind Direction	Anegada Wind	Sea	h	Lapse rate of temp. T	Lapse rate of virt. temp. T*	Lapse rate of mixing ratio w	LCL
	LST		° from N	° m/sec		m	°C/100m	°C/100m	$\times 10^9$cm^{-1}	m
March 18	1450	Cloudy area.	23	18 4	Calm. No whitecaps.	686	.94	.98	29	500
March 21	1400	Cloudy area.	83	93 5	Small waves. No whitecaps.	450	.93	M	M	500
March 25	1115	Cloudy area.	90	89 10	Large waves. Rough whitecaps everywhere.	550	.82	.90	28	655
March 30	1112	Clear area near edge of cloudy area. High cirrus pres.	Estimated 110	110 5	Medium waves. Some whitecaps.	382	.95	.97	28	450
April 1	1045	Clear area near cloudy. Some cirrus. Cunimb buildups 70 mi. north	130	146 4	Small waves. No whitecaps.	382	.95	.98	7.4	580
April 2	1445	Clear area north of small cloudy area. Some cirrus.	118 (smoke)	120 4	Sea calm. No whitecaps.	570	1.04	1.05	11	760
April 4	1150	Clear area. No clouds except over islands.	140 (smoke)	140 6	Small waves. No whitecaps.	700	.90	.93	13	850
April 5	1300	Clear area. No cu except over islands. Middle clouds 8/10.	130 (smoke)	140 7.5	Medium-small waves. No whitecaps.	446	.67	.76	32	855
April 7	0950	Cloudy area.	88 (smoke)	96 5.5	Small waves. No whitecaps.	666	.91	.98	15	760
Average			101	105 5.7		537	.90	.94	20.4	653

TABLE 2. COMPARISON BETWEEN 1946 (H) AND 1953 (L) MIXED LAYERS

	h	LCL - h	Relative Humidity (bottom)	Relative Humidity (top)	Mixing Ratio (bottom)	Mixing Ratio (top)	Lapse Rate of Mixing Ratio	Lapse Rate of Temperature	Wind		T_{lm}
	m	m	%	%	gm/kgm	gm/kgm	$\times 10^9$cm^{-1}	°C/100m	°	m/sec	°C
April 10–28, 1946(H)											
clear	549	186	71	89	15.0	14.6	− 6.4	.90	87	8.9	25.7
cloudy	620	87	71	91	15.1	14.8	− 4.9	.85	96	9.5	25.8
average	575	150	71	90	15.05	14.7	− 5.8	.88	90	9.1	25.7
March 18–April 7, 1953(L)											
clear	496	204	76	85	15.3	14.4	−18.3	.90	131	5.3	25.6
cloudy	588	14	81	94	15.6	14.2	−24	.90	74	6.1	24.5
average	537	120	78	89	15.44	14.3	−20.4	.90	106	5.7	25.1

virtual temperature excesses of 0.6–0.8° C could rise through about half the depth of the mixed layer before losing their buoyancy at normal rates of mixing. When the lapse rate is 5% superadiabatic, as in the case of April 2, they could rise through its entire depth before losing all buoyancy.

Prior to further comparison of the two series using Table 2, it should be pointed out that of the twenty-five H soundings sixteen were made in clear areas and nine in cloudy, and one or more both clear and cloudy area soundings were made on a single observing day. Furthermore wind and synoptic conditions varied little through the H period so that Table 2 essentially presents for series H a comparison between clear and cloudy area soundings at a single time. The temperature difference in the last column therefore probably means that at 11 m elevation the air was slightly warmer in cloudy zones than in clear zones. In series L, soundings were made in cloudy areas whenever any were easily accessible to the aircraft. The five soundings entitled "clear area" were made on days when oceanic cloud groups were small and far between or absent altogether*. Except for the very last day, namely April 7, 1953, the good trade cumulus days were confined to the beginning of the period, and in all cases confined to days when the flow happened to be from east or north of east. The days of poor convection (except for the somewhat anomalous case of April 1) were those in which the flow was from a direction well to south of east. This is reflected in the last two columns of Table 2, which shows a wind averaging 57° more southerly and an 11 m air temperature 1.1° C warmer on poor days for convection.

The most significant difference between the H and L subcloud air lies in the vertical moisture distribution. In series H the mixing ratio hovered about a constant value with height, dropping only about 0.4 gm/kgm from the bottom of the mixed layer to its top. In series L, the air is wetter at the surface, drier at the top, and the mixing ratio lapse rate exceeds that of H by an average factor of 3.5! The character of the vertical moisture structure was quite different in the two series and was even recognizable on the plots of mixing ratio against height. A typical example from each series is reproduced in Figure 6. It appears that in the L series the water vapor just was not getting pumped up through the subcloud layer and it therefore accumulated in the lowest levels. This may, in turn, have inhibited further evaporation. From the effect of higher relative humidity alone, the evaporation rate in series L would have been only 80% that of series H and if Riehl's (16) suggestion is correct, it may actually have been less than 50%. A possible oceanographic consequence of a "stopping down" of evaporation is discussed in the conclusion.

That turbulence in the subcloud layer was below normal in series L has been suggested by Bunker (2) from his low values of shearing stress, turbulent velocities, and eddy viscosities. What proportion of this subnormality of turbulence is attributable to reduced wind stirring and what proportion to diminished heating from below as a result of the changed air trajectories cannot be assessed from these data. The importance of wind stirring in regulating the features of low-level trade-wind air is suggested, however, by two further calculations. The first is presented in the third column from the left in Table 2. This gives the difference in height between the lifting condensation level, LCL, and the top of the mixed layer, h, broken down again into clear and cloudy area categories. In the series H cloudy areas, the top of the mixed layer averaged 87 m below the height of the LCL. In series L, this difference was only 14 m. The buoyancy available to bubbles was nearly the same in both cases and, if anything, greater in L. It seems likely, therefore, that the greater stirring by the wind was responsible in H for subcloud eddies being carried 87 m above the top of the mixed layer to reach saturation. In L the cloudy region LCL and the top of the mixed layer are, with observational error, equal so that no overshooting is indicated.

Finally, Table 1 shows that during the L period large variations in wind speed and temperature lapse rate occurred and an inverse relation between these variables is indicated. This correlation coefficient is, in fact, −0.68, even when corrected for the small number of observations. Despite the dubious representativeness of winds from even such a small island as Anegada (2 by 10 miles), this result suggests that the transports of heat and moisture are greatly dependent on wind

*On April 1, 1953, enormous cumulonimbus build-ups were visible about seventy miles north of the observing area. The ordinary trade cumulus groups were, however, widely spaced and not well developed.

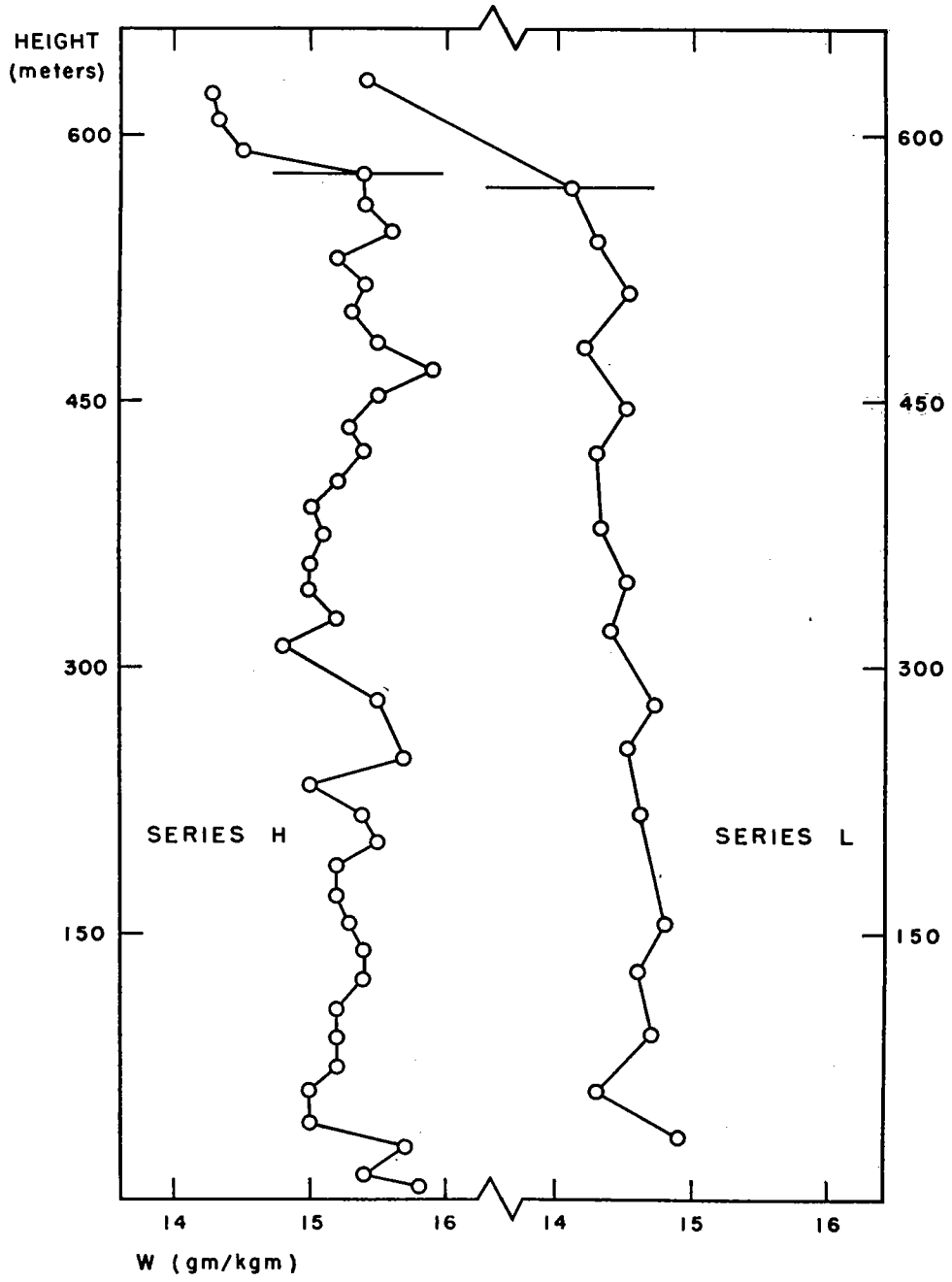

FIGURE 6. Typical plot of mixing ratio against height for series H (left curve, from sounding at 1524 hours LST, April 10, 1946) and series L (right curve, from sounding of April 2, 1953). Both soundings were made in the clear and show nearly equal depth of the mixed layer (solid horizontal line marks its top). The average moisture lapse rate in the L case is 2.5 times that of the H case and its fluctuations about the average are smaller. The latter remains true even when data points from both (continuous) soundings are read off at identical height intervals.

stirring and may become considerably deranged after prolonged periods of subnormal winds. The reality of this inverse correlation between subcloud stability and wind speed is further argued by examination of the average structure of the low-level Pacific trade (18). As the current flows southwestward and accelerates, the mean subcloud lapse rate goes over from slightly superadia-

batic at latitude 32°N to subadiabatic by latitude 21°N despite constant or even increased heating from below. The average wind speed increases by about 0.8 m/sec and the positive wind shear doubles during that travel. Further tests of this relation will be possible in the Atlantic trade following the establishment of a surface vessel making wind and temperature soundings on a routine basis.

Concluding Remarks

The suggestion that important fluctuations in the atmospheric energy supply accompany changes in trade regime has received observational support at the first step, namely, that from the ocean surface to the lowest air and upward through the first few hundred meters.

Returning to the questions raised at the beginning of this section: Concerning the sensible heat fluxes we have as yet said nothing, although some indirect deductions will be made in Parts II and III. Moisture input from the sea and its upward transport through the subcloud layer proved deficient in series L relative to series H, reduced evaporation resulting from higher low-level humidity in L, perhaps augmented greatly by lack of whitecaps. Reduced upward transport resulted from weak and southerly flow, the former giving less sea surface roughness and weaker internal forced stirring and the latter perhaps being responsible for weakened convective-turbulence at very low levels due to (presumed) reduction of the air-sea temperature difference.

One reason why the period March 30–April 7, 1953 was poor for cumulus convection in the observing area has been found, namely, on "poor cloud days" the mixed layer top fell short of the condensation level by more than 200 m. Oceanic warm spots of at least 0.4° C would be required to thicken the layer by that amount (11) and so far such large amplitudes have rarely been observed in the open sea. Thus the initial formation of small oceanic cumulus clouds appears to be controlled largely by processes in the subcloud layer. To understand their further growth, and to inquire why the few trade cumuli that did form during the L period were poorly developed, we must study the structure of the cloud layer itself. This is the subject of Part II.

PART II
ON THE STRUCTURE OF THE TRADE-WIND CLOUD LAYER

The Questions Raised

In this section we wish not only to ask why trade cumuli were better developed in series H than in series L, but to broaden the base of the inquiry to consider the role of cumulus convection in the maintenance and structure of the moist layer as a whole. We begin with an examination of the cloud layer during series H.

The Cloud Layer During a Period of Strong Trade Regime

In series H, conditions varied little during the observing period. Soundings in both clear and cloudy areas were usually made near together on the same day. Therefore mean clear and cloudy area soundings constructed from the entire series are meaningful, useful in defining terms and in illustrating the structure of the moist layer under conditions of strong trade. These mean soundings, constructed by forming averages for each layer rather than at fixed heights, are presented in Figure 7. The typical cloudy area sounding (7A) shows a well-mixed layer averaging 625 m in depth, with a temperature and virtual temperature lapse rate 85% and 87% dry adiabatic, respectively. The mixing ratio decreases about 0.3 gm/kgm from 15 m to the top, which is the same as the magnitude of its average fluctuations. Cumulus base averages 80 m above the top of the mixed layer, defined as in Part I by a sudden increase in mixing ratio lapse rate and a slight stabilization of temperature lapse rate, which is much more pronounced in clear areas than in cloudy.

The cloud layer is defined for both clear and cloudy areas as the region extending from the condensation level up to the base of the trade-wind inversion, regardless of whether the cloud tops are found below or above. In the cloud layer, the lapse rate of temperature, virtual temperature,

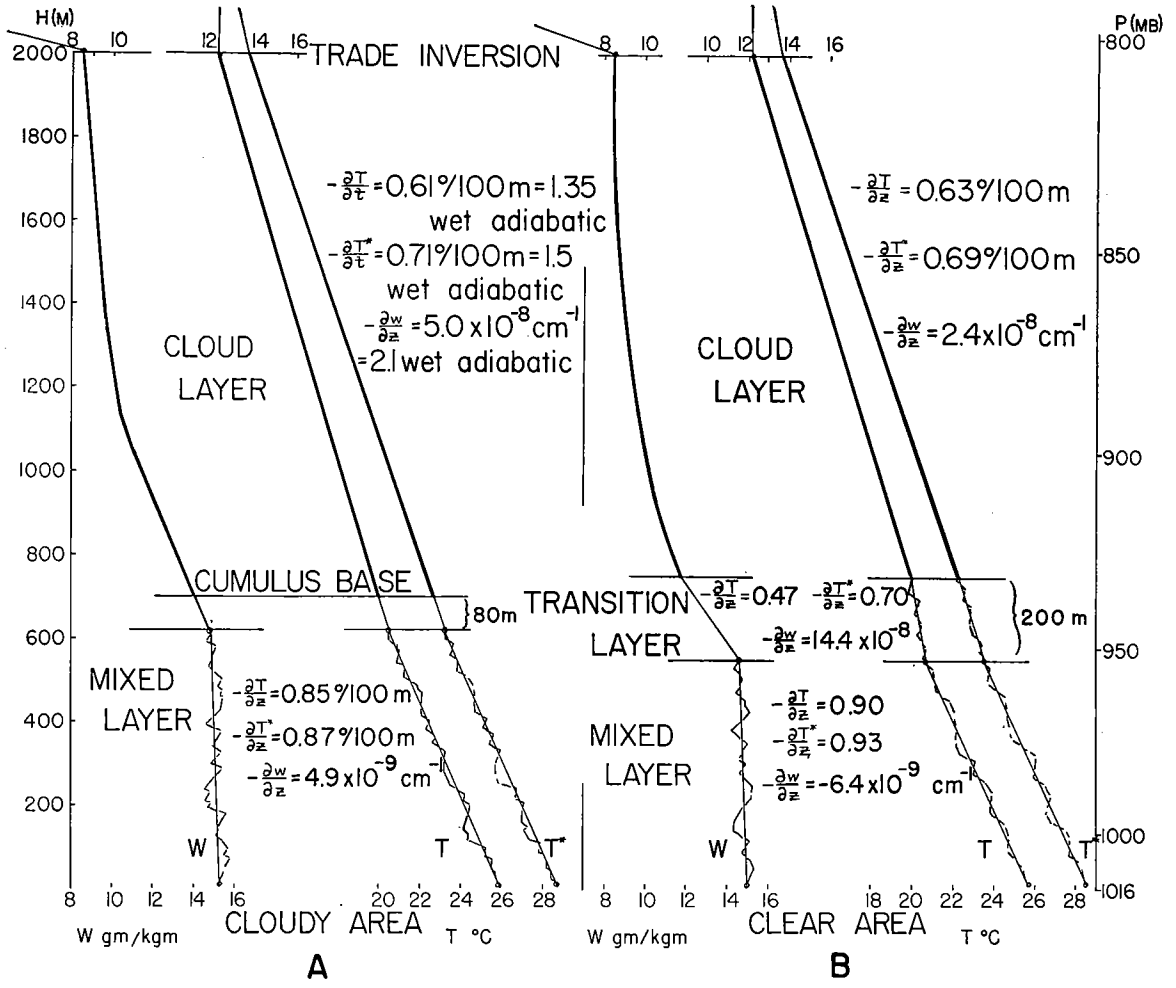

FIGURE 7. Average soundings for H period, compiled by taking the average temperature, T, virtual temperature, T*, and mixing ratio, w, at the base of each layer (see text), the average lapse rate within the layer of each property and the average vertical thickness of the layer. Height in meters is the ordinate. Figure 7A is the average cloudy area sounding (compiled from nine individual soundings) and Figure 7B is the average clear area sounding (compiled from sixteen individual soundings). Generally one or more soundings of each type was made on a given observing day.

and mixing ratio are just in excess of moist adiabatic. A significant feature of the cloudy region cloud layer is that the moisture lapse rate in the upper two-thirds averages only 28% that of the lower third, which may thus be regarded as an extended (about 400m vertical extent) transition zone between unsaturated and saturated convective regimes. The trade inversion is defined by an abrupt increase in moisture lapse rate by a factor of about five and a concomitant stabilization in temperature lapse rate.

In clear areas (Figure 7B) the mixed layer is 75 m shallower than in cloudy areas and has a 15% steeper moisture lapse rate and 6–7% steeper temperature and virtual temperature lapse rates. The main distinction between clear and cloudy soundings lies, however, in the presence of a pronounced shallow transition layer between the mixed and cloud layers. This zone was studied by Bunker et al. in (4) who called it the "stable layer". Re-examination of the data in the light of present knowledge has suggested some revisions in nomenclature and interpretation. The "transition layer" will be defined as a narrow stratum just below or above the height of cumulus base in which the moisture lapse rate is not less than

twice the average in the cloud layer and an order of magnitude greater than that in the mixed layer below, while the temperature lapse rate is concomitantly more stable than the average for either mixed or cloud layer. Due to rapid drying, the virtual temperature lapse rate is generally rather steep in the transition zone, of the order of its magnitude in the cloud layer. The latter led to the preference for the term "transition" rather than "stable" layer. Using these criteria, we found that a transition layer was always (100%) present in clear zones and generally (55%) absent in cloudy ones. In clear zones, it averaged 200 m in depth, had a moisture lapse rate 22.5 times that in the mixed layer, and temperature and virtual temperature lapse rates 47% and 70% dry adiabatic, respectively. In the cloud layer, the temperature and virtual temperature lapse rates differed by only about 3% between clear and cloudy zones, but the moisture lapse rate was half as great in clear areas as in cloudy, partly because in the clear the most rapid drying was confined to the narrow stratum defined as a separate transition zone. Interpretation of these distributions in terms of mechanism will be attempted in Part III. Here we will present the data and some calculations therefrom for the transition and cloud layers of the series H (1946) soundings.

For each sounding, the temperatures, virtual temperatures, and mixing ratios were plotted against height and the vertical extent of the transition and cloud layers was determined according to the above definitions. The average lapse rate of temperature, T, virtual temperature, $\overline{T^*}$, mixing ratio, w, and average relative humidity, $\overline{rh}$, were carefully evaluated for each layer as a whole. The results for all the soundings are presented in Table 3 (p. 46) and are summarized in Table 3A.

The criteria stated previously for the transition layer were met in only four out of nine cloudy area soundings. In four of the remaining five a layer of either somewhat more stable temperature lapse rate or somewhat steeper moisture lapse rate intervened between the top of the mixed layer and the main body of the cloud layer. These cases are included in the averages in Tables 3 and 3A. The problem may be summarized for the present by saying that the transition is much more sharply confined to a limited height in clear spaces and gradually spread out over the lower 400 m or so of the cloud layer in cloudy spaces. The reasons for this will be examined in Part III.

The faster upward decrease of moisture in cloudy areas than in the clear appeared intriguing. It was necessary to determine whether this resulted primarily from the spreading out of the transition zone through the lower cloud layer in cloudy areas. The cloud layer was therefore divided into thirds for each sounding and the moisture lapse rate, $-\partial w/\partial z$, calculated separately for each height interval. The results are summarized in Table 4.

TABLE 4. MOISTURE STRUCTURE OF CLOUD LAYER BROKEN DOWN INTO HEIGHT INTERVALS

Series H

$-\partial w/\partial z \cdot 10^8$ cm^{-1}

	Lower Third	Middle Third	Upper Third
Av. Cloudy....	8.8	4.8	0.3
Av. Clear.....	2.9	0.5	−0.8
Overall Av.....	5.6	2.5	−0.2

(saturated adiabatic $-\partial w/\partial z \cdot 10^8$ cm$^{-1} \leqq 2.4$)

TABLE 3A. SUMMARY OF TEMPERATURE AND MOISTURE STRUCTURE OF TRANSITION AND CLOUDY LAYERS

Series H

	Transition Layer						Cloud Layer						
	Depth m	$\Delta\Theta$ °C	$-\partial T/\partial z$ °C/100m	$-\partial T^*/\partial z$ °C/100m	$-\partial w/\partial z \cdot 10^8$ cm^{-1}	$\overline{rh}$ %	Depth m	$-\partial T/\partial z$ °C/100m	$-\partial T^*/\partial z$ °C/100m	$-\partial w/\partial z \cdot 10^8$ cm^{-1}	$\overline{rh}$ %	Height Trade Inversion m
Av. clear	197	1.6	0.47	0.70	14.4	81		.63	.69	2.4	76	
Av. cloudy	138*	0.4	0.79	0.995	9.0	88		.61	.71	5.2	79	
Overall Av.	177	1.2	0.57	0.80	12.6	84	1328	.62	.70	3.5	77	2080

*Effectively or totally missing in 5 cases out of 9. Average given for 8 cases out of 9. See text.

The marked difference at all levels between clear and cloudy areas is believed to be a significant key to the processes at work in the trade-wind moist layer and will be dwelt on in detail later. Further comparisons between clear and cloudy areas may now be used to resolve a previously disturbing paradox.

All evidence points to mean convergence and ascent in cloudy regions. Despite this, many observers have brought back persuasive evidence that, level for level, cloudy areas are colder than nearby clear areas. Some have brought back measurements made inside tropical cumuli showing that the clouds they observed were colder and denser than the surrounding air. The conclusion has been sometimes ventured, therefore, that tropical cumulus and cumulus groups must be thermally indirect circulations, running against negative buoyancy, and drawing energy from the kinetic energy of the overall flow by some form of convergence therein. That deduction probably contributed to the philosophy of the general circulation which requires that the trades be maintained by energy conversions outside the tropics. Energy would be exported from the trades exclusively in latent or potential form and converted elsewhere. External circulations were hypothesized to maintain the kinetic energy of the trades, which in turn maintains the upward latent energy transport. The grounds for this view collapsed when it was shown in (18) that the pressure gradients maintaining the trades are created by energy conversions within them, but the paradox concerning the cloud groups apparently heightened, since it was shown that the cumulus populations were responsible for the net non-adiabatic heating which maintained these pressure gradients! Fortunately enough data have now been gathered to resolve this difficulty.

It is first necessary to establish whether or not cloudy areas indeed average, level for level, both cooler and denser than the surrounding clear spaces. The 1946 data provide this opportunity. There were eight observing days in relatively undisturbed, well-developed trade on which soundings were taken nearly simultaneously in contiguous clear and cloudy areas. Average cloud layer temperatures, virtual temperatures, and mixing ratios were calculated for the same height interval of each sounding on a given day and the values for clear and cloudy areas compared, first considering cloudy area soundings made outside actual clouds. On seven of the eight days the cloudy areas were colder than the clear by an average of 0.34°C. Since cloudy area soundings averaged 1 gm/kgm wetter than clear, virtual temperatures were next compared. The air near the clouds was denser than that in clear areas on six out of eight cases and averaged a virtual temperature of 0.27°C less than the clear. Considering the in-cloud soundings themselves, clouds averaged 0.4°C colder than clear areas, 2 gm/kgm wetter and had an average virtual temperature *within computational error* of the clear area mean for the same day, individual cloud soundings ranging from about 1°C virtually colder to 2°C virtually warmer. Clearly, cloud virtual temperatures could be and often were warmer than the immediate surroundings but colder than the clear areas. Since the expedition deliberately tried to select active clouds, it seems proven beyond doubt that averaged space-wise, cloudy areas are both colder and denser than nearby clear areas in the undisturbed trade, regardless of the exact proportion of cloud to clear in cloudy areas. This conclusion is supported by later trade cumulus data obtained by the Woods Hole Oceanographic Institution, using both time-lapse photography and individual cloud traverses in which simultaneous temperature, moisture, and vertical motion profiles were made in selected clouds.

Cloudy areas average about a 50% cloud cover. Of the area covered by clouds, about one-tenth is occupied by actively rising towers with a 1–2°C positive virtual temperature anomaly, another one-tenth by actively descending downdrafts with a virtual temperature deficiency of about 1°C, and the remaining cloud matter is weakly negatively buoyant ($\Delta T^* \leqq 0.1$°C) so that, space-averaged, cloudy areas have a virtual temperature deficiency of 0.1–0.3°C. Since all evidence points to mean ascent in the cloudy regions, the existence of the paradox seems confirmed. However, the individual cloud cross sections point the way out of the confusion. On examining simultaneous virtual temperature-draft profiles, we find that on no occasion was an active updraft negatively buoyant.

Some rising, negatively buoyant portions of clouds were observed, but in each case the updraft was decaying with height or time. *A cloudy area is*

composed of a small fraction of actively buoyant, rapidly rising updrafts, a comparable small fraction of strongly sinking, negatively buoyant downdrafts, and a great predominance area-wise of decaying cloud matter and weakly subsiding, slightly negatively buoyant air. Some few of these cloud cross sections have been published (7, 8) and the remainder are on file at the Woods Hole Oceanographic Institution. The following approximately representative figures in Table 5 resolve the paradox.

TABLE 5. DISTRIBUTION OF DRAFTS, VIRTUAL TEMPERATURE, AND MIXING RATIO ANOMALIES WITHIN A CLOUDY AREA

Category	Fraction of Cloudy Area	Draft cm/sec	Mixing Ratio Anomaly (versus clear) gm/kgm	Virtual Temperature Anomaly (versus clear) °C
Active updraft	1/20	+330	+2.3	+2.0
Active downdraft	1/20	−150	+2.1	−1.0
Inactive cloud matter	4/10	− 5	+1.7	−0.1
Clear spaces between clouds	5/10	− 4	+1.3	−0.3
Space average		+5cm/sec	+1.5gm/kgm	−0.14°C

The studies of individual cumuli quoted here have been made almost entirely in the undisturbed trade, or at least not in the near vicinity of pronounced or deep disturbances (from which we are just beginning to obtain cloud penetrations). With this reservation, it may be concluded that trade-wind cumulus and cumulus groups are thermally direct motion systems, running on buoyancy obtained from release of latent heat. The impression to the contrary probably arose from the sampling problem (difficulty in aircraft penetration of an active cloud) and from a faulty averaging procedure, understandably arising from a lack of draft measurements to correlate with those of temperature and humidity.

The corollary paradox of how a net non-adiabatic heating of trade-wind air is produced by flow through cloudy zones themselves level for level both potentially and virtually colder than their surroundings is now resolvable, but its discussion is reserved until Part III.

In Part I it was shown that air near the ocean surface averaged about 0.1°C warmer in cloudy regions than in clear. At the same time the series H observations showed slightly greater stability in the cloudy region subcloud layer, suggesting that the temperature excess was even a bit greater at cloud base. A study of cloud base level properties confirmed this, showing an excess temperature of 0.2°C, excess moisture of 1 gm/kgm and excess of virtual temperature of 0.4°C in cloudy zones (away from actual clouds) compared to clear. Evidence published in (11) accounts for the excess moisture in cloudy zone subcloud layer in terms of gradual circulations of a 10–50 km scale, which appear to be associated with warmer regions in the ocean below. Accounting for the excess temperatures at cloud base in cloudy zones will not prove so straightforward and will be attempted here. Vertical motions on the scale associated with cloud groups were deduced of the order of 4 cm/sec upward in cloudy areas at cloud base level. Thus if this ascent were adiabatic we should expect cooler rather than warmer air at cloud base. For cloudy zones of 10–20 km horizontal dimension the cooling should amount to roughly 0.1°C. Since instead we observe relative warming of about 0.2°C, considerable non-adiabatic heating is suggested. The phrasing is made in this way because we know from the data in (17) that the trade-wind subcloud layer is accumulating rather than losing sensible heat as it flows downstream (at a rate in the Pacific of about 0.6°C per day). The present data therefore suggest that near cloud base the warming is occurring more rapidly in cloudy than in clear areas, which in fact must be cooling at this level to give a reasonable net heating downstream. A warming of 0.3°C in 4,000 sec (roughly the time for the trade to traverse a cloudy area) is much larger than the daily rate of non-adiabatic heating required to overcome radiation loss, leaving a net potential temperature increase of about 0.6°C per day.

We may now inquire how a large warming at cloud base in cloudy areas could be caused. If real, it must be the result of a sensible heat flux convergence. This may be accomplished by radiation, or by motions on a turbulent eddy (50–150 m) scale or a cloud group scale (about 10–50 km) or

some combination. Due to lack of knowledge, we shall unjustifiably ignore radiation (implicitly assuming that the radiative fluxes vary little at this level between cloud and clear) and inquire into the other two processes. The alternatives are an upward decrease of upward heat flux or a downward decrease of downward heat flux. The evidence greatly favors the latter. Recent measurements (from a 1956 expedition to the area, not yet completely analyzed) indicate that above 30 m or so eddy sensible heat fluxes are downward, of about 10–15% the size of the upward latent heat fluxes. While the flux due to the 10–15 km scale motion is probably upward, the sign of its divergence at cloud base is doubtful. Even if negative, a stretching of plausible figures could account at most for one-half of the observed warming. On the other hand, fragmentary observations suggest that the convergence at that level of downward eddy flux is of the correct sign and magnitude.

The model suggested by these data is as follows: Some of the condensation heat released in the cloudy zone cloud layer is transported down the potential temperature gradient (downward) by eddy fluxes, which decrease rapidly through cloud base level toward the surface. In the intervening clear spaces the downward fluxes through the subcloud layer are roughly the same, while the downward flux through the cloud layer is much smaller (due to absence of turbulence away from clouds) and so a flux divergence occurs near cloud base, cooling the air at that level. The net downstream warming indicates that the cooling between cloudy areas is smaller than the warming in cloudy areas and that most of the subcloud layer is warmed indirectly by precipitation heating. These statements should be regarded as hypotheses only, to be tested further both observationally and theoretically, and are not intended to be generalized to all portions of the trades. Supplementary evidence is presented in Part III, where it is shown that convective precipitation in the cloud layer may warm the air sufficiently to overcome radiation losses and provide enough sensible heat excess to be transported down through cloud base level by turbulence.

The Cloud Layer During a Period of Weak Trade Regime

During series L the striking visual difference (as recorded by human observer and aircraft nose camera) from the cloud layer of series H was the sparseness of trade cumulus groups. There is also some evidence that the L period cumuli were weaker and more poorly developed. Comparison of cloud photographs (example in Figures 8A and 8B) suggests that the 1953 cumuli were generally less well organized aggregates of fragments and bubbles, while those of 1946 were more often organized into sturdy-looking vigorous chimneys. Due to the sampling problem and to the lack of actual draft measurements in 1946, however, this deduction is somewhat subjective.

In 1953 only one sounding was made on each observing day, and therefore clear and cloudy areas cannot be compared as was done for 1946. The L soundings were made in cloudy areas on those days when trade cumuli were well developed enough for cloud groups to be easily accessible to the aircraft and in clear regions on those days when trade cumuli were sparse or absent. Thus the 1953 data were used in Part I to compare the mixed layer structure on favorable versus unfavorable days for cumulus. The sparseness of cumuli in the L series proved explainable in terms of processes occurring below cloud. On poor convective days the absence of wind stirring and diminished evaporation restricted the height of the mixed layer well below the condensation level and suppressed the turbulent upflux of moisture through it. This was so pronounced on the two poorest convection days (April 4 and 5, 1953) that no trade cumulus at all were observed over the oceans. In the more than one hundred days that the group has observed in the area, such total absence of oceanic clouds was never duplicated.

The transition and cloud layers for the 1953 period have been analyzed in Table 6 and are summarized in comparison with the 1946 figures in Table 6A.

The striking feature of Table 6A is the similarity of the average figures for the two periods, particularly for the cloud layer. In series L, the transition layer was totally missing in all but one of the cloudy soundings; in that one it was effectively missing. In the clear soundings it was shallower and had a much greater moisture and virtual temperature lapse rate, which in three cases was 96% dry adiabatic or greater, while the temperature lapse rate itself averaged only slightly less stable than in series H. Those properties calculated in the table for the cloud layer are almost

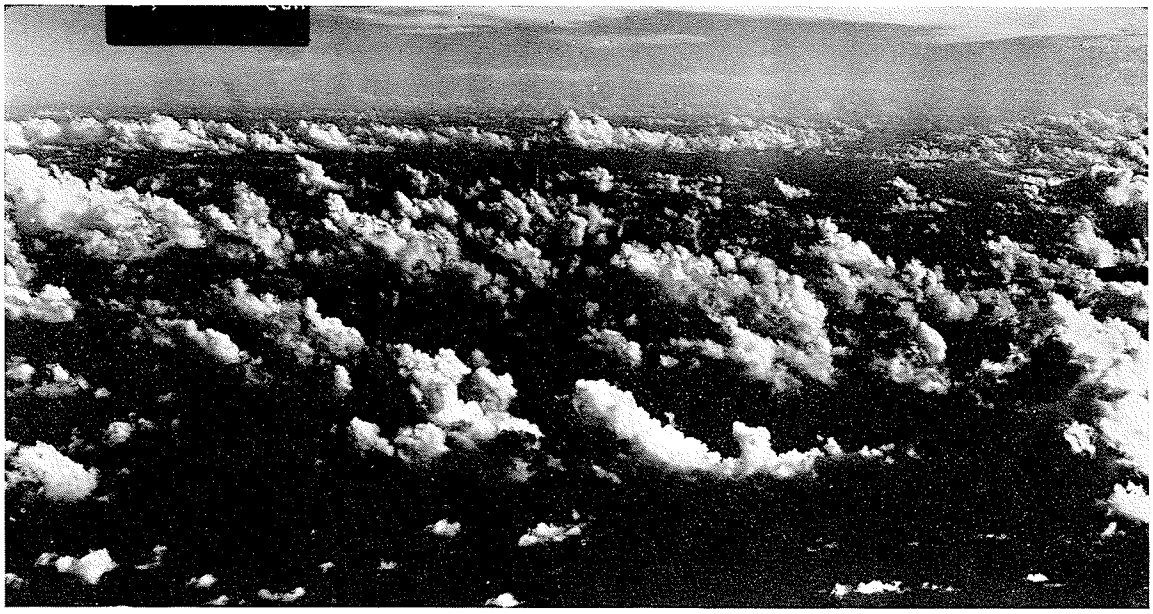

FIGURE 8A. Typical trade cumulus cloud photograph of the H period, made on April 25, 1946, from 20,000 feet altitude. The wind blows from left to right and decreases upward. Note the many vigorous looking chimney-like clouds.

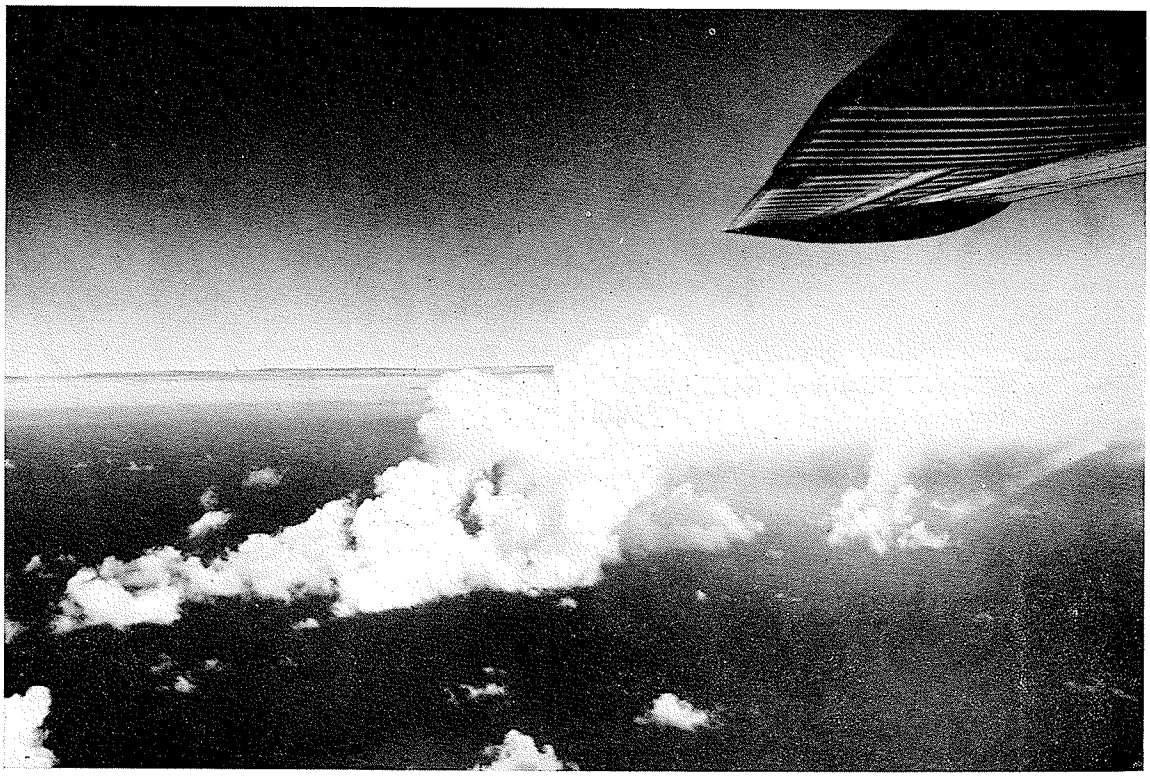

FIGURE 8B. Typical trade cumulus cloud photograph of the L period, made from 6,500 feet on March 21, 1953, looking north so that the trade blows from right to left. The trade inversion is at 2 km (about 6,500 ft.) and the cauliflowerlike top of the cloud is penetrating the drier air. The shelf to the right is formed by spreading of the cloud matter, primarily downstream, just below inversion base. The "black stratus" in the background was formed in a similar manner. Although this was one of the best days for trade cumulus during the entire L period, the cloud has a holey, fragmented appearance typical of that observation series. The top continued growing even after the lower portions had almost entirely dissipated.

TABLE 6. STRUCTURE OF TRANSITION AND CLOUD LAYERS FOR SERIES L (1953) SOUNDINGS

	Transition Layer							Cloud Layer						
Date	Estimated Planetary Divergence 10^6 sec^{-1}	Depth m	$\Delta\theta$ °C	$-\partial T/\partial z$ °C/100m	$-\partial T^*/\partial z$ °C/100m	$-\partial w/\partial z \cdot 10^8$ cm^{-1}	$\overline{rh}$ %	Depth m	$-\partial T/\partial z$ °C/100m	$-\partial T^*/\partial z$ °C/100m	$-\partial w/\partial z \cdot 10^8$ cm^{-1}	$\overline{rh}$ %	Height Trade Inv. (m)	Remarks
March 18 cloudy	1.6			Missing				1311	.59	.65	5.8	90	1835	Uniform cloud tops 1600 m.
March 21 cloudy	−0.1	120	0.9 Layer	0.5 effectively	0.54 missing	6	93	1430	.51	.63	4.2	73	2000	
March 25 cloudy	.07			Missing				1520	.50	.58	2.8	83	2074	
March 30 clear	− .73	188	0.4	0.8	0.96	9	91	3232	.49	.53	2.3	82	3900	Most disturbed day Polar trough. Rain. Cb buildups
April 1 clear	−1.4	190	0.4	0.79	0.97	10	82	906	.56	.69	6.1	79	1350	Multiple inversion. Cb buildups
April 2 clear	− .86	125	1.3	.16	.56	25.6	78	950	.61	.66	1.8	67	1650	Multiple inversion
April 4 clear	−2	90	0.8	0.44	0.89	38	77	977	.71	.77	3.2	77	1767	Worst trade Cu day
April 5 clear	−2.5	30	+0.3	0.33	1.00	40	72	880	.77	.78	2.0	79	1356	Next worst trade Cu day
April 7 cloudy	−0.2			Missing				880	.50	.55	5.8	75	1453	Uniform cloud tops
Av. clear	125	0.6	.51	.88	24.5	80			.63	.69	3.1	77		
Av. cloudy				Missing					.52	.60	4.6	81		
Overall Average	125	0.6	.51	.88	24.5	80		1343	.58	.65	3.6	79	1932	

TABLE 6A. COMPARISON OF SERIES L AND H TRANSITION AND CLOUD LAYERS

	Transition Layer						Cloud Layer					
	Depth m	$\Delta\theta$ °C	$-\partial T/\partial z$ °C/100m	$-\partial T^*/\partial z$ °C/100m	$-\partial w/\partial z \cdot 10^8$ cm^{-1}	— rh %	Depth m	$-\partial T/\partial z$ °C/100m	$-\partial T^*/\partial z$ °C/100m	$-\partial w/\partial z \cdot 10^8$ cm^{-1}	— rh %	Height trade inversion m
1946 clear	197	1.6	.47	.70	14.4	81		.63	.69	2.4	76	
cloudy	138	0.4	.79	.995	9.0	88		.61	.71	5.2	79	
overall	177	1.2		.80	12.6	84	1328	.62	.70	3.5	77	2080
1953 clear	125	0.6	.51	.88	24.5	80		.63	.69	3.1	77	
cloudy			Missing					.52	.60	4.6	81	
overall							1343	.58	.65	3.6	79	1932

identical for the two periods. On the three worst days for trade cumulus convection, namely April 5, 4, and 2 (in that order), the cloud layer was somewhat shallower, drier, and less stable than the average for either year. These differences must be regarded as consequences rather than causes of poor cumulus development, since on two of those days no oceanic clouds whatsoever were observed. If we break down the cloud layer moisture structure by height intervals (Table 7) and compare with series H, we find some differences. These are, as will be seen in Part III, probably also consequences of poor convection.

TABLE 7. MOISTURE STRUCTURE OF CLOUD LAYER BROKEN DOWN BY HEIGHT INTERVALS

Series L

$-\partial w/\partial z \cdot 10^8\ cm^{-1}$

	Lower Third	Middle Third	Upper Third
Av. Cloudy ...	4.7	5.1	5.9
Av. Clear.....	3.5	2.3	5.8
Overall Av. ...	3.6	3.6	5.8

So far all the evidence confirms the conclusion of Part I that the major reason for the sparseness of trade cumuli in the L period is to be found in the subcloud layer. The mechanisms suggested there for its shallowness and ineffective transports concerned a combination of weak and southerly flow, the former removing wind stirring and surface roughness; the latter reducing the air-sea moisture and temperature difference (the last was a supposition with no direct evidence to check it). One further important untested mechanism remains: namely, divergence in the large-scale flow. Divergence has been indicated as a major brake upon convection; it acts to bring down drier air, to stabilize, and to widen the spaces between updrafts. When produced offshore of a heated island (horizontal scale smaller than synoptic, magnitude of divergence about ten times synoptic scale) it creates wide cloud-free rings (9) primarily by lowering the top of the mixed layer below the condensation level. Thus we must consider whether synoptic-scale divergence may not have contributed to a shallower mixed layer during the "poor convection" period of the L series.

If we could ignore the relative vorticity compared to that of the earth, the planetary divergence is estimated from the expression

$$\mathrm{div}_2\mathbf{v} = -\frac{\beta}{f}v$$

where $\mathrm{div}_2\mathbf{v}$ is the horizontal velocity divergence; β is the rate of change of the Coriolis parameter, f, with latitude; and v is the meridional wind velocity, positive from the south. These results have been entered for each day in Table 6. Examination of the synoptic charts for the period suggests that these values are probably of the correct sign, although a more accurate study should be undertaken in a situation where the curvature of air trajectories is calculable. On the disturbed days of March 30 and April 1, the actual

convergence was probably about double that given, due to a contribution from cyclonic curvature in the flow. Surprisingly enough we find the opposite of what might have been expected, namely, an apparently inverse relation between synoptic-scale convergence and the development of trade cumuli. This puzzling result is clarified, however, by further consideration. It must be recalled that we have been studying the oceanic trade-wind cumulus cloud and not land cumulus nor large oceanic towering cumulus or cumulonimbus. The oceanic trade cumulus may be defined as a species of cumulus ranging from about 100 m–2 km across, 300 m–3 km in vertical thickness, possessing updrafts from 0.5–5 m/sec and exhibiting the typical appearance shown in Figures 2 and 8. We saw that the formation of these is largely controlled by the subcloud layer, which in the cases studied was most favorable when the flow was rather strongly from north of east. This maximizes evaporation and upward vapor transport by wind stirring, surface roughness, maximum air-sea temperature and moisture contrast. With those conditions favorable, the trade cumuli seem to function quite well in the face of the average divergence of about $10^{-6}cm^{-1}$ (descent roughly 0.1 cm/sec). If, however, the divergence is stepped up by an order of magnitude, as just seaward of a heated island or ahead of a strong easterly wave, trade cumuli are suppressed either through the shrinkage of the mixed layer or a stablization of the lower cloud layer or both.

Oceanic cumulonimbus build-ups, however, seem to be definitely associated with synoptic-scale convergence produced by travelling disturbances. On the most disturbed days of the L period (March 30 and April 1) cumulonimbi were common over the oceans but the ordinary trade cumuli were very poor. April 1 is particularly interesting. A large line of precipitating cumulonimbi 100 miles east-northeast of Puerto Rico were studied in detail in (12). These clouds reached an elevation of nearly 50,000 feet, were 9 km across, and the towers had measured ascent rates of 12 m/sec. At the same time, ordinary trade cumuli were sparse and poorly developed; the aircraft had insurmountable difficulties in obtaining cross sections through any one before it dissipated. If indeed oceanic trade cumulus and cumulonimbus are to some extent mutually exclusive (this is clearly not always so since a good mixed layer and large-scale convergence may often coincide, as frequently observed in the summer season) a very important question is raised, namely, what fraction of tropical oceanic precipitation falls from trade cumulus and what proportion only from cumulonimbus under disturbed situations? This question has considerable implication for the maintenance and steadiness of the trades and cannot be resolved from land observations, or even those from rather small islands. Tropical island precipitation patterns are controlled by interaction of island effect and trade flow. Their diurnal cloud production is extremely sensitive to convergence in the large-scale flow. Over islands such as Puerto Rico or Jamaica, in the dry season anyway, even the mountain cumuli rarely reach the cumulonimbus or precipitation stage without the help at least of a weak synoptic disturbance. This observation has been summed up quantitatively over a number of years by Riehl (15) who shows that 50% of the precipitation of Puerto Rico comes from 10% of the days on which rain fell. The present study suggests the desirability of similar inquiries about the patterns of tropical oceanic rainfall.

We may now attempt to learn something of the dynamics of the 1953 trade cumulus clouds. It has frequently been stated that on a given day the tops of oceanic clouds are randomly varied downward from the tallest which reach or overshoot the level of zero buoyancy for undilute cores. The reason for the spectrum of heights has been sought. Fortunately the 1953 data were supplemented by a complete series of wide-angle motion pictures obtained from the nose of the aircraft during each sounding, on which heights were noted at frequent intervals. A study of these films was made to relate the height of cloud tops to the features of the sounding. For the region and times studied, no continuous spectrum was found on any one day. Masses of small cloudlets generally occupied the lower third of the layer, with their tops at the first rapid drying, ranging from 700–1,200 m. Tops of medium and larger clouds were generally found associated with regions of rapid drying higher up. On a few occasions when the moisture lapse rate was small and constant, tops of the sizable clouds were rather uniformly near the inversion base. On other occasions two or three levels of cloud tops were found within the cloud layer. These were

readily identifiable as regions of marked drying on the sounding. Those clouds which terminated at a given dry layer were almost invariably smaller in cross section than those attaining the next higher level. A very small fraction of the biggest clouds, probably about one-tenth of the active population, penetrated a few hundred meters into the inversion layer. In general, however, cloud top distribution gave the impression of a series of steps rather than a Gaussian curve. This means, of course, that actively rising towers are rare, and that the growth phase of each cloud is short compared to the mature and dissipating period, as already indicated in Table 5.

Another significant point arising from comparison of the sounding records with the films concerns very moist strata of air that were often found near the inversion base or sometimes well above it, giving the impression of a multiple inversion. The films showed that these were associated with thin stratus streamers spreading out from the tops of cumuli. Langmuir (during a lecture at Woods Hole in September, 1956) proposed that this spreading of cumulus tops is important in lateral moisture transfer; it will later be re-examined in that light.

The impression that the cumuli observed during the L series contained weaker and less well organized updrafts than those of the H series has not yet been analyzed. It may have arisen entirely from the sampling problem, in that the sparseness of clouds often forced the observers to settle for any they could find, or that the few active ones were so far away that they began to die before the aircraft penetrated them. In all the cases studied in this report, the variations in cumulus development, both between series H and L and within series L itself, cannot be explained by changes in cloud layer stability, which if pronounced would surely affect cloud development. However, the average cloud layer stability was only about 17% greater in the H series cloudy areas than those of L, and within the L series itself the poor convection days actually showed lower cloud layer stability than the good ones. Thus we may consider the comparisons undertaken here as a partially controlled experiment in which we investigate the role of factors other than stability in trade cumulus development.

One factor believed to inhibit cumulus development is strong wind shear. Proper wind data were not available for the H period, for the San Juan radio winds were considered neither safely representative of the observing area nor detailed enough. We can, however, compare the wind structure on the good and poor convection days of the L series. In 1953, the British group obtained frequent double theodolite pilot balloon runs from the small island of Anegada (18°50′N; 64°20′W), so that a detailed wind sounding was generally available within a twenty mile distance and one hour time intervals from the aircraft sounding. The wind observations and shearing stresses calculated therefrom have been discussed by Charnock, Francis, and Sheppard (5). Although even such a small island produces a marked sea breeze, its effect on the vertical shear will have diminished by the height of cloud base. Furthermore, we shall be comparing wind fields within the 1953 sounding series, which were all taken near the middle of the day so that the sea-breeze effect should be approximately constant. Table 8 summarizes the wind structure for the L period cloud layer, the values given in each case being taken from the run nearest in time to the aircraft sounding.

The most striking difference between the good convection and poor convection days (average cloudy versus average clear in Table 8) lies in the height of maximum wind and the shear in the lowest 100 m of the cloud layer, which are probably closely related. The mean wind shear in the whole cloud layer averaged around 3 m sec^{-1} km^{-1} for both subgroups, and the best day for cumulus (March 18) had a very large mean shear. The shear in the lowest 100 m of the cloud layer, however, averaged greater by a factor of three on the poor days for convection. On these days, the trade-wind maximum fell considerably below cumulus base and the shear in the lower cloud layer was strongly negative. On the good days for cumulus (except April 7) the wind maximum was usually near or well above cloud base, so that the lower cloud layer was in the region of minimum shear near the turning point. Re-examination of the aircraft cumulus penetrations suggests that vigorous trade cumuli were generally easy to find on days with weak shear near cloud base, although rather strong shears higher up were not fatally inhibitory. Even April 7 fitted in, because by the time the cloud penetrations were made (a few are published in (8)), the wind maximum was above

cloud base and the wind shear in the lower cloud layer was an order of magnitude less (and of opposite sign) than in Table 8.

Care should be exerted, however, in drawing causal conclusions from the above relations without more controlled and quantitative testing. It may be that strong shear at cloud base level inhibits the organization and aggregation of buoyant cloudlets into larger towers and some theoretical evidence (6) backs this view. It may be, on the other hand, that wind maximum at higher elevation is only part of the complex of

TABLE 8. WIND STRUCTURE OF L PERIOD CLOUD LAYER

Date	Mean Wind Speed V m/sec	Mean Shear dV/dz m/sec/km	Height Maximum Wind m	Shear Lowest 100m Above Cloud Base m/sec/km	Remarks
March 18	4	5	780	+2	Little turning below inversion
March 21	6	1	750	+0.2	Weak shear. Little turning
March 25	10	3	936	0	Little turning
March 30	2	~2	0(?)	?	Very disturbed. Westerlies above 300 m.
April 1	3	3	225	−3.3	Strong veer through cloud layer
April 2	3.5	3	936	−2.6	Wind max. 312 m at 1600 LST
April 4	6	1.7	624	−4	Wind increase through inversion
April 5	2.7	6	312	−9	90° veer upper cloud layer
April 7	3.4	3.5	330	−4	45° veer upper cloud layer
Av. clear	3.8	3.4	524	4.7	
Av. cloudy	5.8	3.1	699	1.5	
Overall Av.	4.8	3.2	611	3.1	

phenomena concomitant with a strongly developed trade situation, other properties of which, such as a good mixed layer, are dominant in determining trade cumulus development.

CONCLUDING REMARKS

We conclude that, at least in undisturbed situations, trade-wind cumuli are thermally direct, buoyancy-driven circulations and that the few active clouds in a group can be virtually warmer than their nearby surroundings, while the group as a whole usually is, level for level, potentially and virtually cooler than the adjacent clear spaces.

In comparing the poorer development of cumulus in series L with the good convection of series H we find that the relative sparseness of cumuli in L was due primarily to conditions below cloud, namely, a shallower mixed layer with deficient upward moisture flux. The impression that the existing cumuli in L were weaker than those of H, if true, could not be attributed to changes in cloud layer stability, which varied little. The difference in cumulus development between the good and poor convection days within series L may have been compounded by markedly stronger wind shear in the lower cloud layer on the poor days.

As far as the runaway growth of cumuli to precipitating cumulonimbi is concerned, all these factors may be little relevant compared to large variations in stability or moisture content produced by synoptic scale convergence. The implications of this question in overall trade-wind dynamics will be considered further in Part III.

PART III
A PHYSICAL MODEL OF THE MOIST LAYER

A physical model describing the processes at work in the cloud layer will be constructed here, primarily for the strong trade situation in which transports by trade cumulus convection are operating vigorously. The aim will be to explain the distributions observed in the mean soundings for cloudy and clear areas (Figures 7A and 7B) in terms of mechanism and thus to illuminate the role of the moist layer in the fuel supply for larger-scale circulations.

Moisture Transport and Its Mechanisms in the Cloud Layer

In (4) a first orientation calculation was made to account for the moisture distribution in the cloud layer in clear areas. In the clear zones two processes were hypothesized to be transporting moisture, namely, small-scale turbulence carrying it upward and cloud-group-scale subsidence (compensating for the net upward motion in cloudy areas) carrying it down. The authors assumed, for want of better information at that time, that the observed nearly steady distribution was achieved *in situ* by a balanced opposition of these two processes. The subsidence rates and eddy transport coefficients obtained were consistent with the observed moisture gradients and of plausible size. It was tacitly assumed in (4) although not stated, that any net upward flux of vapor was achieved in cloudy areas, the transports in which were not treated then due to insufficient knowledge about cumulus convection.

Observational material obtained since permits us to modify and extend the earlier work to construct at least a crude model of clear and cloudy areas together. A large fraction of this material comes from studies of the northern Pacific trade. A vertical section along a trajectory in (17) shows that the lower trade accumulates vast quantities of latent heat in flowing downstream. Numerically, the amount is enough to deepen the moist layer by 1 km in 2,500 km horizontal travel, and at the same time increase its average mixing ratio by about 1 gm/kgm. In combination, this means that an average air parcel increases its mixing ratio by about 0.6 gm/kgm per day. A budget study of this Pacific section showed that the accumulation was achieved by a convergence of upward moisture flux in excess of that required for precipitation. Those calculations showed that only about three-fourths of the water evaporated from the sea surface was carried upward through cloud base, and only about one-fifth that evaporated escaped upward through the inversion. Thus about 25% of the vapor evaporated was exported downstream in the subcloud layer. In the cloud layer, about one-half the gain (55% that evaporated) was recondensed and precipitated and one-half exported downstream. The Pacific study further showed that cumulus convection alone was easily adequate for the net upward vapor flux through mid-cloud layer and to account for the downstream rise in height of its upper boundary. This picture can be extended and filled in from our more detailed data on the Atlantic trade, provided we can carry over the rough framework of the Pacific flux distribution. This is, on the average, clearly well justified since the evaporation rates in the two regions are closely similar and in both regions only a small fraction of the evaporated moisture escapes upward through the inversion base in undisturbed situations. Although this fraction reaching the upper troposphere in the poleward half of the trade is undoubtedly of considerable importance in the long run, we shall set it equal to zero for the present first orientation, thus assuming that all the moisture evaporated is accumulated in the moist layer, and to maintain the steady state, either precipitated there or exported downstream. This implies an upward diminution in net upward moisture flow, roughly as outlined in Table 9.

Table 9. Approximate Vertical Distribution of Net Upward Moisture Flux

Evaporation from sea surface	$\leqq 6.0 \times 10^{-6}$ gm cm^{-2} sec^{-1}
Flux upward through cloud base level	$\leqq 4.5 \times 10^{-6}$ gm cm^{-2} sec^{-1}
Flux upward through inversion	~ 0

In attempting to explain the moisture distributions of Figure 7 in relation to these net fluxes, we must recall that in the cloud layer, small-scale turbulence is observed only in nearby association with active or recently dissolved clouds. This leads to the following formulation, with which any physical or mathematical description of the cloud layer must be consistent: Eddy turbulent transport is of small importance in clear areas. In cloudy areas it is of importance mainly as a brake upon convection and in exchange of properties between clouds and surroundings. Vertical transports are effected by cumulus and cumulus group scale motions. This will guide us to a model describing the transfer of water and heat from cloudy to clear zones independent of strong lateral mixing and dependent only upon convective circulations superposed on the trade-wind flow. Thus, for present purposes, use of eddy exchange coefficients for the cloud layer will be avoided and attention is concentrated instead upon fluxes and gradients, using our physical deductions about the cloud layer to explain these mechanistically.

We shall first show that the upward moisture flux occurs entirely in cloudy zones and that the vertical flux in the clear is probably downward. For series H the average mixing ratio in the cloudy zone cloud layer was 11.6 gm/kgm while that in corresponding clear zones was 10.1 gm/kgm. If clear zones average 1.5 times the area of cloudy, the average descent rate in the clear (from Table 5 to meet continuity) is 3.3 cm/sec. Thus the net upward moisture flux near the middle of the cloud layer is

$$\overline{A_c\rho_c W_c w_c} - \overline{A\rho W w} = \text{net upward flux} \qquad (1)$$

where the subscript c denotes cloudy area properties and the symbols without subscripts refer to clear area properties. The A in each case is the fraction of the total area; ρ is the air density; W is the vertical velocity in cm/sec; and w is the mixing ratio in gm/gm. The left side of (1) can be crudely approximated by

$$\overline{A_c\rho W}_c\overline{w}_c - \overline{A\rho W}\,\overline{w} \backsimeq 0.4 \times 10^{-3} \times 5 \times 11.6 \times 10^{-3} - 0.6 \times 10^{-3} \times 3.3 \times 10.1 \times 10^{-3} = 23.2 \times 10^{-6} - 20.0 \times 10^{-6} = 3.2 \times 10^{-6} \text{ gm cm}^{-2} \text{ sec}^{-1} \qquad (2)$$

which compares well with the average between cloud base value of 4.5×10^{-6} gm cm^{-2} sec^{-1} and cloud top value of zero (Table 9). However, it may be objected that setting $\overline{\rho_c W_c w_c} \sim \overline{\rho W}_c \overline{w}_c$ suffers from the same averaging difficulties discussed in Part II, where we showed the serious error in equating $\overline{WT^*}$ to $\overline{W}\,\overline{T^*}$, except that in the case of moisture flux the result of (2) must be at least qualitatively correct since even the driest air (between clouds) in cloudy zones is moister than the clear. Indeed, breaking down the cloudy zone flux into transports by strong updrafts, strong downdrafts and weakly subsiding air using Table 5 gives a net flux similar to but somewhat larger than that of (2), a small difference between large upward transport in cloudy areas and nearly equally large downward transport in intervening clear spaces.

More physical insight, however, is gained if we subdivide the cloud layer vertically into thirds and discuss the flux distribution in terms of gradients of w and W, referring back to Table 4. Table 9 suggests that there is a net flux convergence in the cloud layer averaging about 3.4×10^{-11} gm cm^{-3} sec^{-1}, that is, if uniform, the net upward flux would decrease by 1.5×10^{-6} gm cm^{-2} sec^{-1} in each third (about 430 m height interval) of the cloud layer. If, as other evidence suggests, the mean ascent rate in the cloud layer increases upward slightly between cloud base and the middle of the cloud layer and then decreases rapidly toward the inversion, we can readily see the necessity for a rapid upward moisture decay in the lower cloud layer, superseded by a more gradual one higher up. For the upward flux to decrease from cloud base to mid-cloud layer in the face of constant or increasing upward motion, rapid drying must occur. Similarly, subsiding clear areas must average drier than cloudy for a net upward flux and must dry more slowly with height for a smaller flux divergence. A quantitative breakdown of fluxes as a function of height is attempted in Table 10.

In Table 10, the average vertical motion distribution in cloudy areas was estimated from Table 5 and evidence in (11) that it increases from about 3–5 cm/sec at cloud base to a maximum somewhere between 1–1.3 km elevation and then decreases to about zero by inversion base. The mixing ratios are the observed means from series H soundings. The total net flux convergence arrived at in Table 10 agrees well with the cruder estimate in Table 9. Since nothing about mechanism has been said, these calculations cannot be regarded as an "explanation" of fluxes or gradients even if these rough figures prove accurate. They

TABLE 10. CALCULATED MOISTURE FLUXES AS A FUNCTION OF HEIGHT IN CLEAR AND CLOUDY AREAS

	Estimated Vertical Velocity $\overline{W}$(cm/sec)		Observed Mixing Ratio w(gm/kgm)		Flux $\rho\overline{W}w \cdot 10^6$ gm cm^{-2} sec^{-1}		Flux Convergence · 10^6 gm cm^{-3} sec^{-1}		Flux Convergence · 10^6 Times Fraction Total Area		Net Flux Convergence · 10^6 in Height Interval
	cloudy	clear	cloudy	clear	cloudy	clear	cloudy	clear	cloudy	clear	
Cloud base	+5	−3.3	14.2	12.4	+71	−40.9					
							7.4	−2.1	7.4 x 0.4 = 2.96	−2.1 x 0.6 = −1.26	1.7
One-third way up in cloud layer	+6	−4	10.6	9.7	+63.6	−38.8					
							35.7	−21.4	35.4 x 0.4 = 14.3	−21.4 x 0.6 = −12.8	1.5
Two-thirds way up in cloud layer	+3	−2	9.3	8.7	+27.9	−17.4					
							27.9	−17.4	27.9 x 0.4 = 11.2	−17.4 x 0.6 = −10.4	0.8
Inversion base	0	0	~8.5	~8.5	0	0					
											Total flux through cloud base = flux convergence = 4.0 x 10^{-6} gm cm^{-2} sec^{-1}

merely show that the assumption that the Atlantic trade is accumulating moisture in a similar way to the Pacific trade is consistent with both observed gradients and plausible estimates of vertical motions. The latter will be used later in a discussion of mechanism.

The outstanding feature of the moisture transports in the cloud layer as deduced is the large up-and-down flux and flux convergence compared to the net transport. The calculated upward transport in cloudy areas exceeds the evaporation rate by an order of magnitude. It appears that the moist layer is carrying out a large internal re-arrangement of water vapor for a small net gain. Actually, a fairly straightforward interpretation of this flux distribution is possible in terms of the scales of motion operating, which forms part of a mechanistic model relating many features and processes in the trades. It will be described here, with the reservation that it is not so firmly established at present that alternatives may be ignored. Reasonably enough, our physical interpretation of the results of Table 10 (and of many other properties of the moist layer) depends upon our views concerning the structure and life cycles of trade cumulus populations, and strangely perhaps, primarily upon whether or not these populations move along with the trade or whether the air moves through them. The alternative models which can be used in accounting for the fluxes of Table 10 are as follows:

1. Individual cloud groups are stationary or moving downstream very slowly so that the trade flows on the average through them, first undergoing a net rise and then a nearly equal net subsidence (ignoring the overall mean subsidence of about 0.1 cm/sec as much smaller). A mean trajectory would look like the sketch in Figure 9. If trajectories everywhere coincided with mixing ratio isopleths, Table 10 would be superficially little changed, except that the small net flux convergence in the last column would disappear. Moistening at each level would occur in cloudy zones due to convergence and ascent; divergence and descent would undo this in the clear. Actually, the small net accumulation must

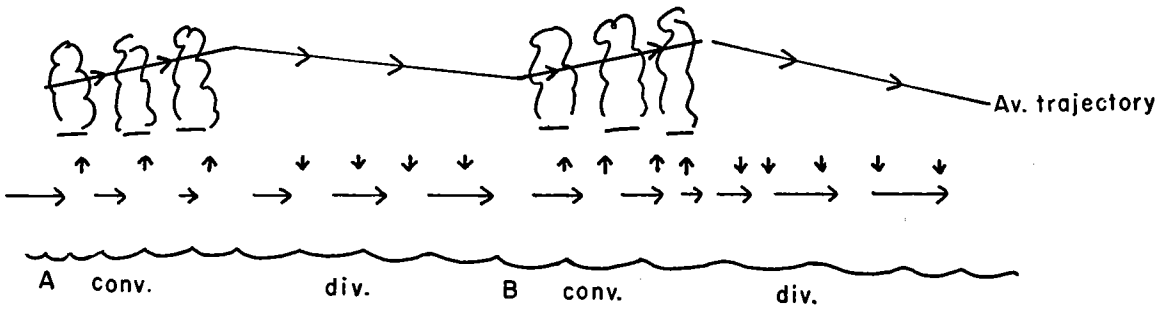

FIGURE 9. Schematic cross section through the moist layer in the plane of the lower trade based on the assumption that cloud groups are stationary or move downstream more slowly than the wind. The solid line (with arrowheads) is an average trajectory, which ascends in cloudy areas and descends an equal amount in the clear.

show up as a slight crossing of trajectories toward higher mixing ratio in cloudy zones, the two sets of lines becoming parallel on the descent portion in the clear, so that at B the air at any level is wetter than at A (corresponding level).

2. No relative motion occurs between individual cloud groups and trade winds, but new cloud groups break out and die at rather rapid intervals randomly as the air flows downstream, so that an average trajectory would still look qualitatively like the sketch in Figure 9, with more irregular amplitude and spacing of ascent and descent, but still with a hypothetical typical air parcel spending about four-tenths of its time in cloudy regions and six-tenths in the clear.

3. Cloud groups occupy the same air for a long time in its travel downstream so that an average air parcel might make one or several complete circuits from the base of the cloud layer to its top and back to the base in clear as the cloudy zone drifts with the wind. This would require that the same air be occupied by cloud for a major fraction of twenty-four hours; to produce the observed lapse rates of temperature and moisture, saturated ascent, mixing, and condensation are required in cloudy areas, and nearly saturated descent with evaporation and mixing are required in the clear. Extended influx of clear air into cloudy regions is necessary near cloud base and horizontal, quasi-laminar efflux from cloudy regions at the top of the cloud layer.

4. Cloud groups occupy the same air for long periods and impart moisture and other properties to the clear by lateral mixing.

Model 4 may be discarded without further discussion due to the absence of turbulence in clear areas. Model 3 may be discarded, although less categorically, because in undisturbed situations it is doubtful whether evaporation and nearly saturated descent can occur far from clouds; it thus becomes difficult to avoid very high stability and low moisture in the clear. Nevertheless, one of this model's required mechanisms, namely quasi-laminar efflux of moisture from cloud groups at high levels, will be reconsidered later in a different connection.

We are therefore led to conclude that in the cloud layer moisture is communicated between cloudy and clear areas — i.e., their structure differs as little as it does — because any given batch of air alternates frequently between being clear and being occupied by cumuli. Whether this is achieved by the trades flowing through more slowly moving cloud groups, or whether each cloud group drifts with the wind in its lifetime and when it dies a new group forms in different air remains to be seen. A quantitative development of Model 1 will show that it accounts simply for many features of the moist layer and tentatively suggests its preference over Model 2.

Let us consider that trade cumulus groups are either stationary in space or travelling very slowly downwind, so that the air is moving at roughly 5 m/sec relative to the distribution of clear and cloudy areas. Let us suppose that cloudy areas are 20 km across and clear areas 30 km across. An average trajectory in the middle

of the cloud layer would look something like that sketched in Figure 9, rising about 200 m in the cloudy zone and descending the same amount more gradually in the clear. Of course, any real aggregate of air molecules may go up and down several times in clouds, may rise all the way to the inversion, or may actually undergo continuous descent; the mean trajectory represents only an average which becomes more meaningful the wider the cloud group compared to individual clouds and the longer time spent crossing it compared to their lifetimes.

The first step toward a quantitative model is made as follows: We take the vertical distribution of moisture at the downstream edge of a cloud group as given, established by the convection within the cloudy region and past history of the air. We work out the trajectories at selected levels through the next (downstream) clear area, taking a horizontal velocity of 5 m/sec and the vertical motions given in Table 10. Since the model assumes that trajectories and mixing ratio isopleths nearly coincide across clear areas, we get a section like that shown in Figure 10A.

Only the cloudy area moisture structure and clear area descent rates have been given and yet we arrive at a very realistic clear area moisture structure, averaging drier than cloudy, possessing a rapidly drying transition region in the lower third and an upper portion with a more gradual moisture lapse rate than in cloudy zones, with actual mixing ratio values typical of clear areas. More important, we gain physical insight into the difference between the moisture structure of clear and cloudy areas. If the mean vertical motions first increase with height in the cloud layer and then decrease toward the inversion, the necessity for a stronger decay (transition zone) at the base of the layer and a weaker lapse rate above in clear compared to cloudy follows naturally. The close agreement between clear zone mixing ratios in Figures 10 and 7B suggest that the chosen magnitudes for air motions relative to cloud groups are reasonable.

In Figure 10B, 10A is amended to show a more schematic average trajectory through the preceding (upstream) cloud group, giving a 0.1 gm/kgm increase of moisture on each trajectory during its passage through the cloud group. This is roughly consistent with the net flux convergence in Table 10 allowing for precipitation loss. It may thus be useful to regard the flux convergences calculated in Table 10 as largely the result of mass convergences and vertical motions on a cloud group scale, which on the average cancel as the air moves up and down in passing from cloudy area to adjacent clear. In other words, they appear as a consequence of the upward and downward motions of the air trajectories through fixed levels and would disappear if we followed a trajectory. The important small net flux convergence is more profitably viewed as the slight crossing of the trajectories toward higher moisture which is accompanied by cumulus-scale motions, in a manner we shall attempt to describe presently.

First, however, the numbers in Figure 10B suggest a probable but not conclusive preference of Model 1 to Model 2. If as in the latter, a given cloud group drifted with the air during its entire life, and if the typical lifetime of a cloud group is as long as three to five hours, the vertical amplitude of the trajectories would be so great that the difference between typical clear and cloudy area soundings would be much larger than observed. The loopholes in this argument are still numerous enough to preclude discarding Model 2. They are as follows:

1. The observations of stationary oceanic cloud groups with lifetimes of three to five hours have been made from islands and good estimates of population motions and durations over open sea are not yet available. If the latter should average as short as one or two hours, the trajectory amplitude of Model 2 becomes close to that of Figure 10B and therefore consistent with soundings.
2. The vertical motions used in Figure 10B may conceivably be too large. Their reduction by a factor of two would also bring the trajectory amplitude of Model 2 close to that of Figure 10B.
3. Figure 10B itself may be an understatement of the differences in structure between the downstream end of a cloudy area compared to the downstream end of a clear area, which should be a maximum. The average clear and cloudy area soundings used here were compiled from aircraft ascents located randomly within clear and cloudy areas. Since the mean difference

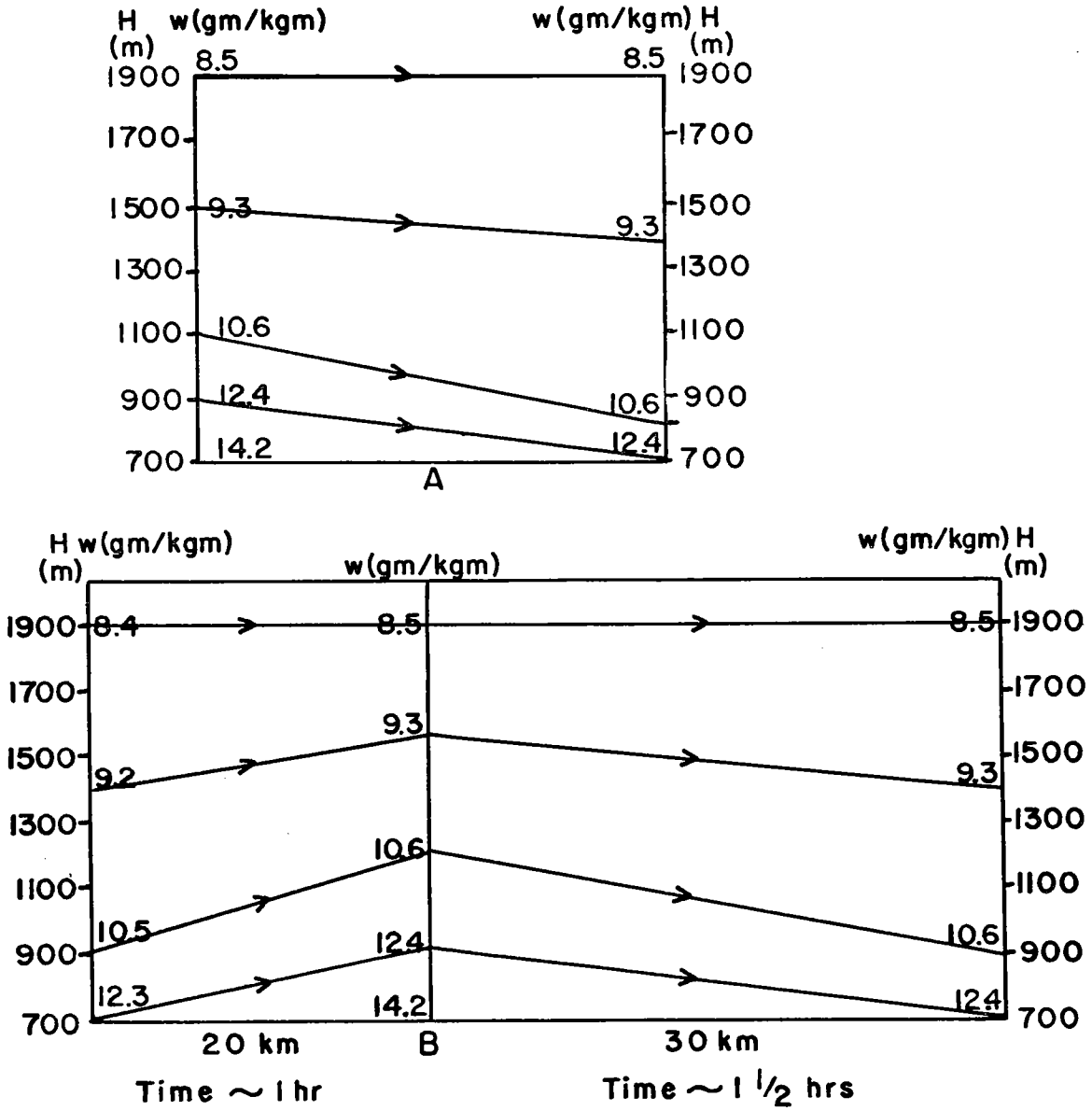

FIGURE 10. Schematic cross section in the plane of the trade wind showing the average trajectories at several heights (solid lines with arrowheads) and distribution of mixing ratio in gm/kgm (numbers with decimal points). Figure 10A shows a clear area. The moisture distribution at its upstream (left) boundary is typical of a cloudy area while that at its downstream (right) boundary has been rearranged by the descent and its height variation to be typical of observed clear area stratification. Figure 10B has Figure 10A as its right-hand portion but adds a cloudy area on the left-hand side. Note the slight increase in moisture along the trajectories in the cloudy areas The times are those which the air would spend crossing an area of the given size if it moved through it at 5 m/sec.

may be considerably less than the extreme at downstream ends, longer average times spent in each time of area than those shown in Figure 10B are not precluded.

Thus the decision between Models 1 and 2 for the undisturbed trade must await further observations, preferably by photography from a stationary ship or tiny atoll. The real situation may lie part way between the extremes, with variations in time and space. In any case, the mean trajectory must qualitatively resemble that of Figure 10B. In many tropical disturbances, such as slow-moving easterly waves, we can be confident that the trade moves westward through the convective zones and

a model of this type will be useful in describing their effect upon the air structure.

The previous paragraphs focus attention on the vertical moisture structure in cloudy areas from which, once established, the distribution in clear areas follows simply. A crude qualitative picture of the maintenance of the vertical moisture structure in cloudy regions is now undertaken, using recently acquired knowledge about the operation of single cumuli and cumulus populations. Figure 7A was compiled from soundings in cloudy areas but away from clouds. The moisture distribution in inactive clouds is nearly the same. Therefore, since clear spaces and inactive cloud matter constitute about nine-tenths of a typical cloudy area, we may consider that the average moisture distribution in cloudy regions is given by Figure 7A. Nevertheless, it is the active clouds which produce this distribution.

From a study of nine cloud cross sections, we find an average vertical moisture lapse rate in active drafts of 3.8×10^{-8} cm^{-1}, with a tendency to be somewhat steeper in the lower and upper portions than in the middle. In the small sample studied, downdrafts showed only a slightly greater drying rate with height than updrafts. This moisture lapse rate, 160% saturated adiabatic, is established by mixing between clouds and surroundings, the dynamics of which is not yet well known and is beyond the scope of this discussion.

The outstanding features of the moisture structure of the cloud layer as a whole are: The large upward gradient in the lower third, of 8.8×10^{-8} cm^{-1} (nearly four times moist adiabatic, which is about 2.4×10^{-8} cm^{-1}), diminishing to about one-half this value in the middle third, and almost vanishing in the upper third. This upward reduction in moisture lapse rate can be explained qualitatively in terms of present incomplete knowledge of cumulus dynamics. A clue to the rapid decrease in the lower third is provided by the photographs in Figures 2 and 8 or in fact by any typical photograph of trade cumuli. For every medium and large-sized cloud, we see great numbers of small cloudlets, only a few hundred meters in diameter and thickness. These are commonly found in the lower cloud layer, often clustered around the bases of larger clouds. It was suggested from observations in (7) that the big clouds, in fact, form from an aggregation of these smaller cloudlets or "bubbles". Time-lapse photographs indicate that the beginning stages of a cloud population consist of a large number of these, formed from condensation in the wetter eddies in the subcloud layer. Cross sections through individual middle-sized trade cumuli showed that below about 1,000 m (above sea level; about 400 m above cloud base) the cloud was composed of several small buoyant elements, which appeared to fuse together into a single more vigorous draft higher up.

The lower third of the cloud layer, then, we may describe as a region of organization, a few strong drafts aggregating from many small cloudlets whose tops vary from heights of about 800–1,100 m. A region of rapid upward drying is associated with each level where cloud tops are found, the trade inversion itself being the most striking. A rough calculation illustrates the point in the lower cloud layer: Let us suppose that there is five-sixths cloudiness at 850 m in a typical cloud group. The cloudy air has a mixing ratio, say, of 13 gm/kgm and the air which has recently been clear has a mixing ratio of 11.2 gm/kgm (Figure 7B). The average is 12.7 gm/kgm. These small cloudlets have a lifetime of five to ten minutes, so that air spending one hour or so in a cloudy area should have experienced about ten of them. Turbulent mixing is relatively strong between them and we find that consequently the moisture fluctuations in a traverse through the lower cloud layer are rather small (about 1 gm/kgm). If at 1,100 m, the active cloudiness is reduced to one-fourth, with clouds averaging 12 gm/kgm mixing ratio and air recently clear, 10 gm/kgm, the average vapor content becomes 10.5 gm/kgm. These figures agree well with cloud cross sections and the mean moisture distributions of Figure 7. It may at first seem contradictory that the lower cloud layer is the region of very rapid upward intensification of active updrafts. The cloud cross sections show that the main updraft in a given cumulus may increase by a factor of three or even five between cloud base and 1 km. However, if the number of updrafts per unit area decreases by almost this proportion, the small calculated increase (about 20%) in net ascent rate between cloud base and 1,100 m is well accounted for. The medium-sized clouds reaching the middle of the cloud layer or higher have lifetimes of fifteen to

thirty minutes, so that an average air parcel may enter only three or four of them during its time spent in a cloudy area. This, plus greatly reduced inter-cloud turbulence aloft accounts for the larger moisture fluctuations (2–3 gm/kgm) on a horizontal cloudy area traverse in the mid-cloud layer, which in fact become even larger as inversion base is approached. The observation that in the mid-cloud layer the overall moisture lapse rate exceeds that in active saturated updrafts by only about 20% suggests that a considerable fraction of the trade cumuli which get above 1,100 m penetrate all the way to the trade inversion, although on individual days regions of rapid drying are often found apparently associated with a "top limit" for certain sizes of clouds. This point cannot be framed more quantitatively at present without more knowledge of cumulus dynamics.

The nearly constant vertical distribution of moisture away from active clouds in the upper portion of the cloud layer is probably produced by the spreading of cumulus tops. Shelves or streamers of stratus emerging from the upper parts of cumuli frequently creep across an entire cloudy area and even far into adjoining clear spaces. They may be composed of water droplets or ice crystals depending on the elevation. The importance of this phenomenon was suggested by Langmuir*. Physically, it is envisaged as a nearly laminar spreading of cloudy matter as it encounters a stable layer. A similar phenomenon was observed in laboratory experiments on convection described in (19). Bubbles of mud slurry were released into a tank of still water. These moved downward due to excess density, diluting on the way. On several occasions the tank contained a lower salty layer which was denser than the bubble fluid so that each element very abruptly encountered a sudden stabilization of its environment. A typical bubble penetrated only a small fraction of its diameter into the stable layer and "fell" back, spreading its material laterally *above* the interface (i.e., on the less stable side). After a few bubbles, the water above the interface became muddied through a considerable depth, while that below the interface remained transparent. It seems likely that a similar mechanism is often at work in the upper trade-wind cloud layer. In this way even in the absence of wind or wind shear, cloud matter can be dispersed to considerable distances. A crude calculation from continuity suggests that if a 2–3 m/sec updraft 1 square kilometer in cross section is killed in 200 m vertical ascent and if the air spreads out in a wafer 200 m thick (this figure is suggested by the depth of moist wafers on soundings and observed thicknesses of the stratus sheets), the horizontal velocity of spreading is roughly 4 m/sec at first, or comparable to the original speed of the updraft. Due to the very low values of turbulent friction near inversion base, cloud matter may thus spread several tens of kilometers before being brought to rest or losing identity by mixing with the surroundings, although the visible water particles may not remain that long. Strong wind shear introduces asymmetry and the spreading in one direction may be greatly emphasized (see Figures 2 and 8B for examples).

The moisture gradients in the upper cloud layer and their variations between clear and cloudy regions are thus qualitatively understandable. In cloudy zones the upward moisture decrease becomes very small as inversion base is approached, but does not vanish because new moisture is continually being supplied from below by cloud activity. In the clear, moisture is not being pumped upward from below and the only source is, in fact, by injections at upper levels from cloudy regions. A slight amount of downward diffusion may actually be occurring in addition to the mean transport downward by subsidence of the air itself. Thus in Figure 10 the upper trajectories should perhaps be crossing moisture isopleths toward higher values even in the clear.

The foregoing discussion treats the strong trade situation with active cumulus convection. Comparing the cloud layer moisture gradients of the L period with those of the H period (Table 7 compared to Table 4), we find that in the period of weak trade and poor convection the moisture lapse rate in the cloud layer was only about 10% steeper than that of the H period, but it was much more uniform in the vertical and actually increased from the middle to the top third of the layer. The physical model evolved here suggests the reason: A smaller fraction of L period cumuli penetrated the upper cloud layer and spread out below the inversion. The 1953 cloud photographs support this explanation.

*In lecture and conversations at Woods Hole during September 1956.

Thus the moist layer in the L period was drier (by an average of about 0.5 gm/kgm) than in the H period. Since the trade was also weaker, the downstream moisture export was also probably much reduced. In the L period a section 1 cm wide and 2 km deep with a wind of 5.7 m/sec and an average mixing ratio of 12.3 gm/kgm exports 140 gm/sec water vapor. The corresponding H period section of the same dimensions (average depths of the moist layer were nearly the same) having a mixing ratio of 12.8 gm/kgm and a wind of 9.1 m/sec would export 233 gm/sec. Although these absolute values are too high, since surface winds were used, the point is made that this portion of the trade exported only about 60% of the moisture in the L period as it did in the H period. This figure agrees well with the estimates in Part I of the reduction in evaporation during the L period. All evidence put together suggests that the Atlantic trade latent heat supply was producing at a significantly reduced rate during at least a month in the spring of 1953. This period of time is long enough and the Atlantic trade a large enough circulation branch to suspect consequences in other portions of the general circulation. It would be desirable to study the same and subsequent weeks in the equatorial and upper tropical Atlantic and even in the westerlies and Pacific trade with this background in mind.

Further insight into the actual process of latent heat accumulation by the trade can be gained by inquiring how the cumuli actually bring it about. We saw that the net accumulation showed up as a crossing of mean trajectories toward higher moisture content so that after each passage through cloudy plus subsequent clear zone, the air returns to its original level slightly wetter than it left. Because of the ascent of the trajectories, air leaving the downstream edge of a cloud group at any level must be about 0.5–0.6 gm/kgm wetter than air at the same level at the upstream edge for individual parcels to have gained 0.1 gm/kgm. It is readily shown that the shedding of moist air from the active cumuli is an adequate supply. If we take the active drafts (up and down) to occupy one-tenth of the area, and if they are about 1 gm/kgm wetter than their surroundings, normal rates of exchange of air or "erosion" of cloudy matter supplies $0.2 - 0.4 \times 10^{-3}$ gm/sec of vapor to a slice of air 20 km long, 1 cm deep and 1 cm thick. If the mass flux through the slice corresponds to a 5 m/sec wind, the air emerges 0.4–0.8 gm/kgm wetter than the air at the same level at the entrance edge. Thus by bringing up wetter air from below and at any given level exchanging some of this with the drier surroundings, the cumuli act as "sources" of water vapor for the trade at each height. We may regard this as the accumulation process in the lower and middle cloud layer.

Near the level of the cloud tops where the moist layer is increasing in thickness, the physical mechanism differs somewhat. In Figure 10, except for the slight moistening of the top streamline we have ignored the downstream increase in depth of the moist layer. As was shown in (17), this occurs in the face of mean subsidence and was related there to the process of convection. If this thickening takes place entirely in cloudy regions, it should average about 20 m in each cloud group. That is to say, a wafer of air just above the inversion base which on entrance dries about 0.5 gm/kgm through its vertical thickness (from about 8.5 to 8.0 gm/kgm) leaves the cloudy area with uniform moisture content. Using the figures presented here, we find that if one-tenth of the active clouds in the mid-cloud layer penetrate a net distance of 20 m into the inversion layer and dissolve there, the required moistening is achieved. Clearly individual towers frequently shoot 300 m or more into the inversion layer and they or their dissolved remnants descend back all or most of the way. It is therefore better to say that the required moistening is achieved if one-tenth of the cloud-matter active in mid-cloud layer, with allowance for dilution on the way, is left above the inversion base in the process of cloud tower dissipation.

Thus the net moistening of the trade stream is easily accounted for by ordinary cumulus convection and it is not required to call upon cumulonimbus build-ups or disturbances to explain the water vapor accumulation and export by the trade. The answer to the question of whether we may ignore these for precipitation is, however, probably negative. A recent study of tropical oceanic precipitation in (1) indicates that the expectation of precipitation from tropical cumuli is less than 50% if their tops are below 3 km, in part because the coalescence process requires a minimum time for droplets to spend in cloud. Leaving precipitation physics outside the scope of this discussion,

however, it is possible to inquire whether ordinary trade cumuli are able to release enough liquid water for the observed mean precipitation, even assuming that the mechanism for coalescence and fallout is always available. To produce the mean daily rainfall of 0.13 cm estimated in (17), each cloud group 20 km on a side must produce about 5×10^{10} gms of precipitation. If active trade cumuli have liquid water contents of 2 gm/kgm (result from unpublished observations at the Woods Hole Oceanographic Institution) and if one-twentieth of the area is occupied by updrafts of 3.3 m/sec, we find that 52×10^{10} gms of water are condensed in the time the air takes in passing through the cloud group. A study of cumulus downdrafts in (8), however, suggests that a very large fraction of the liquid water so released is consumed by evaporation in downdrafts. Nevertheless, since only 10% of the total is adequate for precipitation, we conclude that it is possible for trade cumuli to condense enough water to account for a non-negligible fraction of tropical oceanic precipitation. The crux of whether or not they do contribute this depends upon the physics of the precipitation mechanism and its interaction with cumulus dynamics and thereby with the synoptic situation. If a 3 km cloud depth is indeed necessary for a significant amount of rain, the average undisturbed dry season moist layer of 2 km depth is inadequate, and at least a weak convergence field is needed. This is not necessarily true in the wet season where the undisturbed moist layer is much deeper. We next consider the importance of this question in regard to the non-adiabatic heating of trade-wind air.

The Production of Downstream Warming in the Trades

The trades gain sensible heat as they flow westward and equatorward. We see this in a crossing of the average trajectories toward higher potential temperature, which amounts to about 0.6°C per day in the summer season. Riehl and Malkus showed in (18) that this sensible heat accumulation amounted to 25% of the latent and was responsible for producing the downstream pressure drop which maintains the trades against friction. A heat budget calculation showed that the net warming was accomplished primarily by an excess of precipitation heating over radiation loss and that the sensible heat provided directly by the ocean was small in comparison.

If the addition of heat to the air is accomplished by release of latent heat, it must occur entirely in zones of precipitating clouds. This deduction was apparently paradoxical when compared with the observation that cloudy areas average both potentially and virtually colder than the surroundings. Riehl (14) found this "cold core" particularly pronounced in the convective zones of disturbances. The difficulty is, however, readily resolved if we recognize that, particularly in disturbances, the air moves downstream through the more nearly stationary convective zones: First upward in the cloudy region and then downward in the succeeding clear as sketched schematically in Figure 9. Level for level, therefore, it is potentially and virtually colder within the cloudy zone, but if precipitation occurs the air returns to its initial level warmer than it left. This reasoning can be framed quantitatively for the passage of normal trade-wind air through a group of precipitating cumuli 20 km across followed by a clear zone 30 km across. Figure 11 shows a vertical plot of typical clear and cloudy temperatures and potential temperatures (taken from Figures 7B and 7A, respectively) with the calculated trajectories of Figure 10B superposed. The air ascends in the cloudy region and descends in the clear with the mean velocities of Table 10. *While crossing the cloudy zone the trajectories cross isentropes towards higher potential temperature.* Thus the air cools as it rises, but at a rate more nearly moist than dry adiabatic. If the descent in the clear were isentropic, the air would arrive at its original pressure considerably warmed. The consequent warming as a function of height is plotted on the inset graph at the top of Figure 11. It averages 0.3°C per passage through a cloudy and succeeding clear zone. If the air crosses ten of these in twenty-four hours, it would gain 3°C per day, which allows for approximately 2°C per day radiation loss and 1°C per day left over for net heating in the cloud and subcloud layers. We have discussed earlier the probable downward flux by eddying of part of this heat to warm the subcloud layer and the numbers in Figure 11 are approximately right so that when this gain is redistributed it slightly exceeds radiation loss in the observed manner.

Furthermore, the average precipitation over the tropical oceans when distributed through the cloud layer in roughly the manner of Figure 11 is

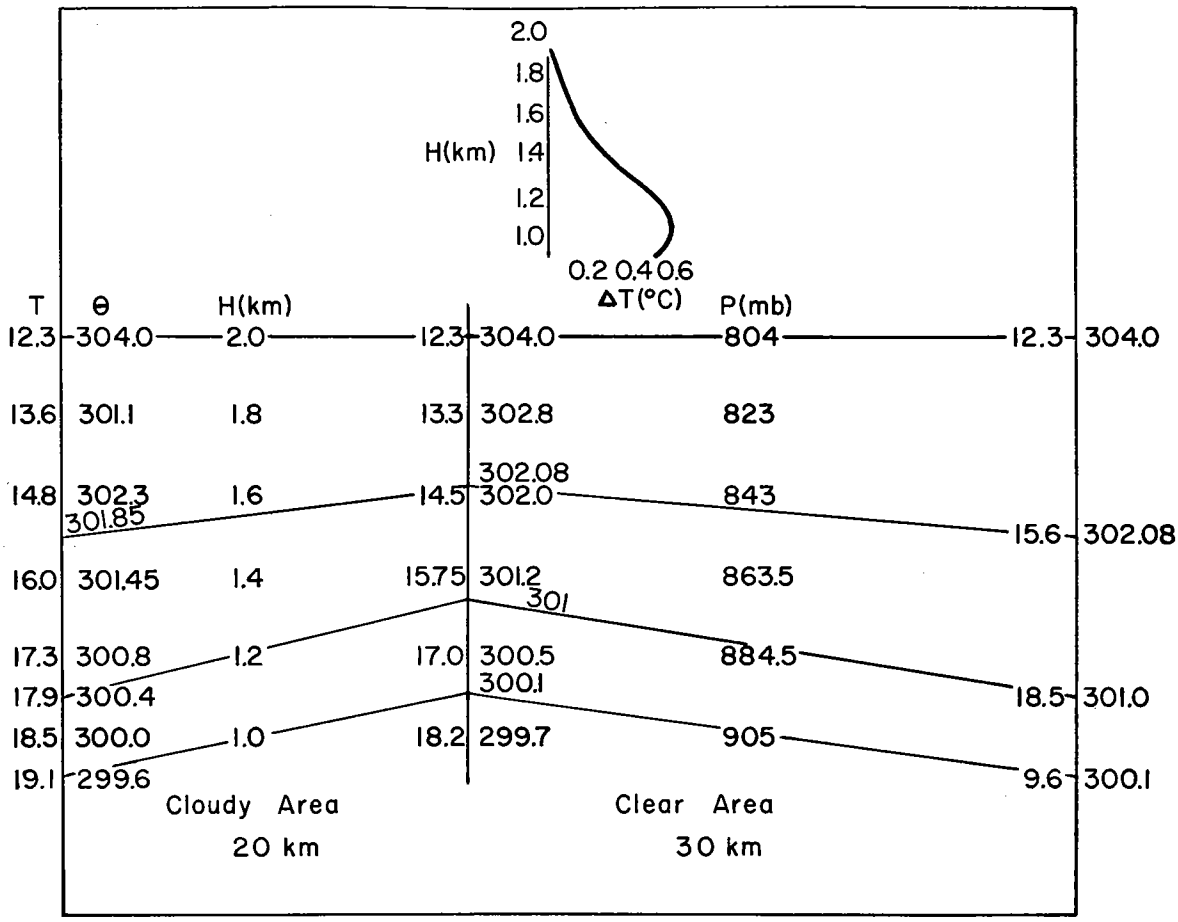

FIGURE 11. The main portion of the diagram is a vertical cross section in the plane of the trade similar to 10B, with the same average trajectories (solid lines with arrowheads). Here the three figure numbers (T) with decimal points (to the left of the vertical solid lines) are temperatures in °C and those to the right (θ) are potential temperatures in °A. The column on the far left (upwind side of cloudy area) was taken from Figure 7B as typical of a clear area and those on the middle vertical (downwind side of cloudy area) are taken from Figure 7A as typical of a cloudy area. Those on the far right (downstream edge of the following clear area) were derived by isentropic descent from the downstream edge of the cloudy region. The graph inset above is the resulting net non-adiabatic warming, or the difference in potential temperature on a given trajectory between the far right and the far left, that is after a complete passage through a cloudy area and the clear area downstream of it.

adequate in magnitude to account for the heating, although it remains to be seen whether Figure 11 applies to areas of typical undisturbed trade cumuli or whether most of the rainfall and heating should be confined to disturbances which would give rarer but much more intense lifting and heating. The proportion contributed by disturbances may differ from dry to wet season and from the upstream to the downstream portion of the trades. That rainfall occurs from ordinary trade cumuli under undisturbed conditions is finally well documented (13) and the Woods Hole group has obtained several cross sections through such clouds which were precipitating heavily. The question has thus resolved itself from "whether" to "how much". It is interesting to note that in the relatively undisturbed H period, oceanic cumulonimbus build-ups were reported on one day (April 23) and swelling cumulus with tops over 6,000 feet on three days (April 23, 27, and 28) in each case associated with a weak trough passing the region (Figure 3A). No information on oceanic precipitation was available. In the L series, precipitating oceanic cumulonimbus were noted on the two most disturbed days (March 30 and April 1) and a large precipitating swelling cumulus reaching 7,000 feet was studied in detail on March 21, on which occasion the trade inversion was found at its normal undisturbed height of 2 km. Further studies of tropical oceanic rainfall in relation to cloud structure and the synoptic picture are greatly needed.

CONCLUSIONS, CONSEQUENCES, AND FURTHER OUTLOOK

THE data studied here indicate that the energy export from a large portion of the trade may vary by a factor of two or more at different phases of the index cycle in the same season. We have suggested some of the atmospheric consequences of this variation; these should be investigated further in the equatorial trough zone and aloft in the tropics where the poleward energy export occurs. Similar studies of the operation and structure of the moist layer are now being undertaken in other seasons and other portions of the trade.

The consequences upon the ocean itself of fluctuations in the trade flow should be examined. One sample calculation illustrates the possible effect of variations in evaporation comparable to those inferred here. If evaporation is cut by a factor of two for a period of ninety days, the sea surface would become about 1.2°C warmer than under normal evaporation, even if the heat loss is distributed through an ocean layer 100 m deep. This temperature rise would be doubled if decreased wind stirring permitted the oceanic mixed layer to shrink to half that depth. A 2°C sea surface temperature difference may be critical in the formation and development of tropical disturbances and in long run energy storage in the oceans. It would be desirable to relate ocean temperatures and effectiveness of storm breeding during a wet season with the trade-wind index over the area during the preceding spring.

Particularly desirable would be a combined meteorological-oceanographic study relating the characteristics of the mixed layers of sea and air, their interactions and how it affects and is affected by larger-scale processes. Such a program is planned by the Woods Hole Oceanographic Institution using research ship and aircraft jointly and it is now in its beginning phases.

ACKNOWLEDGMENTS

This work was supported by the Office of Naval Research who have generously maintained the aircraft, the research staff, and other meteorological facilities at Woods Hole for many years.

The writer wishes to acknowledge the very large contribution made by her colleague, Mr. Andrew F. Bunker, whose studies of the trade-wind mixed layer set the precedent for this work and which promise in the future to resolve many of the questions concerning fluxes and transports which have been left open here.

Many others have contributed to the collection and evaluation of the present data, in particular the crew of the PBY aircraft who many times went beyond the call of duty to obtain successful flight observations. Mr. Claude Ronne ably planned and carried out the photographic program, and Mrs. Mary C. Thayer reduced the data, drafted the drawings and aided in preparing the manuscript.

REFERENCES

(1) BATTAN, L. J., and R. R. BRAHAM, JR., 1956: A study of convective precipitation based on cloud and radar observations. *J. Meteor.*, 13, 587–591.

(2) BUNKER, A. F., 1955: Turbulence and shearing stresses measured over the North Atlantic Ocean by an airplane-acceleration technique. *J. Meteor.*, 12, 445–455.

(3) BUNKER, A. F., 1956: Measurement of countergradient heat flows in the atmosphere *Australian J. of Phys.*, 9, 133–143.

(4) BUNKER, A. F., B. HAURWITZ, J. S. MALKUS, and H. STOMMEL, 1949: Vertical distribution of temperature and humidity over the Caribbean Sea. *Pap. Phys. Oceanog. and Meteor.*, Mass. Inst. of Tech. and Woods Hole Ocean. Inst., 11, No. 1, 82 pp.

(5) CHARNOCK, H., J. R. D. FRANCIS, and P. A. SHEPPARD, 1956: An investigation of wind structure in the trades: Anegada 1953. *Phil. Trans.*, 249, 179–234.

(6) HOLMBOE, J., 1955: On the evolution of symmetric updrafts in a current with constant shear. Dept. of Meteor., U.C.L.A., Final Rep. of Autobarotropic Flow Project Contract No. AF19(604)–728.

(7) MALKUS, J. S., 1954: Some results of a trade cumulus cloud investigation. *J. Meteor.*, 11, 220–237.

(8) ——, 1955: On the formation and structure of downdrafts in cumulus clouds. *J. Meteor.*, 12, 350–354.

(9) ——, 1955: The effects of a large island on the trade-wind air stream. *Quart. J. Roy. Meteor. Soc.*, 81, 538–550.

(10) MALKUS, J. S., 1956: On the maintenance of the trade winds. *Tellus*, 8, 335–350.

(11) ——, 1957: Trade cumulus cloud groups: Some observations suggesting a mechanism of their origin. *Tellus*, 9, 33–44.

(12) MALKUS, J. S. and C. RONNE, 1954: On the structure of some cumulonimbus clouds which penetrated the high tropical troposphere. *Tellus*, 6, 351–366.

(13) PALMER, C. E., J. R. NICHOLSON, and R. M. SHIMAURA, 1956: An indirect aerology of the tropical Pacific. Univ. of California, Inst. of Geophysics. Final Rep. Contract No. AF19 (604)–546. 131 pp.

(14) RIEHL, H., 1948: On the formation of west Atlantic hurricanes. Misc. Rep. No. 24, Dept. Meteor., Univ. of Chicago. pp. 1–67.

(15) ——, 1950: On the role of the tropics in the general circulation. *Tellus*, 2, 1–17.

(16) ——, 1954: Variations of energy exchange between sea and air in the trades. *Weather*, 9, 335–340.

(17) RIEHL, H., T. C. YEH, J. S. MALKUS, and N. E. LASEUR, 1951: The northeast trade of the Pacific Ocean. *Quart. J. Roy. Meteor. Soc.*, 77, 598–626.

(18) RIEHL, H., and J. S. MALKUS, 1957: On the heat balance and maintenance of circulation in the trades. *Quart. J. Roy. Meteor. Soc.*, 83, 21–28.

(19) SCORER, R. S. and C. RONNE, 1956: Experiments with convection bubbles. *Weather*, 11, 151–154.

APPENDIX I

1953 Soundings — Reduced and Tabulated

Temperature, T (°C), mixing ratio, w (gm/kgm), virtual temperature T* (°A), and potential temperature θ (°A) are presented in the following tables as functions of pressure, p (mb), and height (true), h (m), for each of the nine 1953 soundings.

The times and locations of the soundings, the Anegada surface winds and the ambient cloud character are given in the heading to each. Times are in local standard time (LST) which is Greenwich (GCT) time minus four hours.

March 18, 1953. 1450 LST. Sounding in cloudy area.
Wind 18°, 4 m/sec. Location: 5 miles north of Anegada.

p (mb)	h (m)	T (°C)	w (gm/kgm)	T* (°A)	θ (°A)	p (mb)	h (m)	T (°C)	w (gm/kgm)	T* (°A)	θ (°A)
1013.4	15	23.0	15.9	298.9	294.7	903.1	992	14.6	11.4	289.6	296.5
1007.9	55	23.1	15.5	298.9	295.2	899.8	1024	14.6	11.5	289.6	296.7
1004.2	85	22.7	15.2	298.4	295.3	896.5	1056	14.2	11.3	289.2	296.6
1000.4	115	22.3	14.9	298.0	295.3	893.1	1088	14.2	10.6	289.0	296.9
996.9	145	21.9	14.8	297.5	295.2	889.7	1120	14.5	9.9	289.2	279.4
993.4	177	21.7	14.8	297.3	295.3	886.5	1151	14.0	10.6	288.8	297.1
989.7	209	21.3	14.8	296.9	295.2	883.3	1182	13.8	10.7	288.6	297.3
986.1	241	21.0	14.6	296.6	295.1	880.0	1213	13.6	10.6	288.4	297.4
982.7	273	20.6	14.5	296.2	295.0	876.9	1244	13.4	10.4	288.2	297.5
979.0	305	20.2	14.7	295.8	294.9	873.5	1275	13.3	10.5	288.1	297.6
975.5	336	20.0	14.6	295.6	295.2	870.2	1306	13.0	10.5	287.8	297.6
971.9	367	19.7	14.5	295.2	295.0	867.0	1337	12.9	10.4	287.7	298.1
968.4	398	19.4	14.2	294.9	295.3	863.7	1368	12.6	10.2	287.4	298.1
964.9	429	19.1	14.1	294.6	295.0	860.5	1399	12.5	10.2	287.3	298.3
961.4	460	18.9	14.0	294.4	295.1	857.4	1430	12.3	9.8	287.0	298.4
957.9	492	18.6	14.1	294.1	295.3	854.1	1460	12.1	9.5	286.7	298.7
954.4	524	18.4	13.8	293.8	295.1	850.9	1485	11.9	9.7	286.6	298.6
950.9	556	18.1	13.8	293.5	295.3	847.8	1511	11.7	9.6	286.4	298.8
947.4	588	17.8	13.6	293.2	295.4	844.5	1537	11.7	9.4	286.3	299.1
943.9	620	17.5	13.6	292.9	295.3	841.2	1563	11.8	8.5	286.3	299.6
940.5	652	17.1	13.4	292.4	295.3	838.3	1589	11.7	9.0	286.2	299.7
937.0	683	17.0	13.4	292.3	295.6	835.1	1615	11.0	9.6	285.7	299.4
933.6	714	17.0	12.6	292.2	295.7	832.0	1645	11.3	8.5	285.8	300.0
930.1	745	16.5	12.5	291.7	295.6	828.9	1675	11.7	8.0	286.1	300.6
923.3	810	16.3	12.5	291.5	296.0	825.8	1715	11.3	8.0	285.7	300.6
919.9	840	16.3	12.2	291.4	296.3	822.7	1745	11.3	8.0	285.7	300.9
916.6	870	15.5	12.4	290.6	296.1	813.5	1835	10.8	7.0	284.0	301.4
913.1	900	15.8	12.5	291.0	296.7	810.4	1865	10.9	6.0	284.9	301.5
909.8	930	15.4	11.9	290.5	296.6	807.3	1895	11.1	5.0	285.0	302.1
906.5	960	15.0	11.7	290.0	296.6	798.2	2005	11.3	4.0	285.0	303.3

March 21, 1953. 1400 LST. Sounding in cloudy area.
Wind 93°, 5 m/sec. Location: 25 miles north of Anegada.

p (mb)	h (m)	T (°C)	w (gm/kgm)	T* (°A)	θ (°A)	p (mb)	h (m)	T (°C)	w (gm/kgm)	T* (°A)	θ (°A)
1015.8	20	25.8	M	M	297.4	946.3	630	20.8	15.8	296.6	298.7
1013.9	35	25.6	M	M	297.4	942.9	660	20.7	15.8	296.5	299.0
1010.3	70	25.4	M	M	297.5	936.0	720	18.4	10.9	293.3	297.3
1006.6	100	25.1	M	M	297.5	929.1	780	18.4	9.3	293.0	297.9
1002.9	135	24.7	M	M	297.5	925.7	808	18.4	9.4	293.1	298.2
999.3	166	24.6	M	M	297.7	922.3	836	18.1	9.5	292.8	298.3
995.8	197	23.9	M	M	297.3	919.0	864	17.8	9.7	292.5	298.2
991.1	228	23.8	M	M	297.6	915.5	892	17.4	10.2	292.2	298.0
988.5	259	23.4	16.8	299.4	297.4	912.2	920	17.2	10.2	292.0	298.2
985.0	290	23.2	16.8	299.2	297.3	905.5	976	16.7	10.4	291.5	298.3
981.4	322	23.1	16.1	299.0	297.7	902.2	1004	16.6	10.1	291.4	298.5
974.3	386	22.6	17.1	298.6	297.8	898.9	1032	16.4	9.7	291.1	298.7
970.8	417	22.2	17.0	298.3	297.7	895.5	1060	16.1	9.6	290.8	298.6
967.3	448	22.1	17.0	298.1	298.0	892.1	1095	15.6	10.8	290.5	298.5
963.8	480	21.9	16.4	297.8	298.0	888.9	1130	15.2	11.1	290.1	298.4
960.3	510	21.9	16.8	297.9	298.4	885.7	1165	15.1	11.0	290.0	298.6
956.8	540	22.0	16.4	297.9	298.9	882.4	1200	15.1	11.0	290.0	299.0
954.3	570	21.3	16.1	297.1	298.4	879.3	1235	14.9	11.0	289.8	299.0
949.8	600	21.2	16.3	297.1	298.7						

[1] Changed range on psychrograph.

872.6	1305	14.6	10.4	289.4	299.2	840.7	1642	13.8	6.2	287.9	301.6
869.4	1340	14.5	9.9	289.2	299.6	837.5	1673	13.6	5.5	287.5	301.9
866.1	1375	14.5	9.1	289.1	299.8	834.4	1704	13.5	5.2	287.3	302.0
862.9	1410	14.5	8.9	289.0	300.2	831.3	1735	13.4	5.2	287.2	302.3
859.8	1444	14.1	9.7	288.8	300.0	828.2	1766	13.1	5.8	287.1	302.3
856.5	1478	13.8	9.5	288.4	300.0	825.1	1797	12.6	6.7	286.7	302.0
853.3	1512	13.9	8.2	288.3	300.5	822.0	1828	12.7	5.7	286.6	302.5
850.2	1556	14.0	7.1	288.2	301.0	818.9	1859	12.4	6.3	286.5	302.5
846.9	1580	13.9	7.3	288.2	301.2	815.9	1890	12.0	7.1	286.2	302.5

March 25, 1953. 1115 LST. Sounding in cloudy area.
Wind 89°, 10 m/sec. Location: 2 miles north of Anegada.

p (mb)	h (m)	T (°C)	w (gm/kgm)	T* (°A)	θ (°A)	p (mb)	h (m)	T (°C)	w (gm/kgm)	T* (°A)	θ (°A)
1016.5	15	23.0	13.7	298.4	294.6	912.9	915	15.6	11.0	290.5	296.3
1014.6	31	22.5	13.9	298.0	294.2	909.6	946	15.5	10.9	290.4	296.4
1011.0	61	22.3	14.0	297.8	294.1	906.2	976	15.3	10.8	290.2	296.8
1007.3	92	21.9	13.5	297.3	294.3	902.9	1007	15.2	10.6	290.0	296.7
1003.6	122	21.6	13.4	297.0	294.3	899.6	1037	14.9	10.8	289.8	296.8
1000.0	153	21.4	13.3	296.7	294.4	847.6	1525	12.5	9.3	287.1	299.6
996.5	183	21.2	13.3	296.5	294.5	844.3	1556	12.2	8.9	286.7	299.6
992.8	214	20.8	13.1	296.1	294.4	841.4	1586	12.1	9.0	286.6	299.8
989.2	244	20.4	13.0	295.7	294.3	838.2	1617	11.9	9.2	286.5	299.9
985.7	275	20.3	12.8	295.6	294.5	835.1	1647	11.7	8.8	286.2	300.0
982.1	305	20.2	13.0	295.5	294.8	832.0	1678	11.7	8.3	286.1	300.5
978.6	336	19.8	12.7	295.0	294.8	828.9	1708	11.4	8.9	285.9	300.3
975.0	366	19.6	12.6	294.8	294.7	826.0	1739	11.0	8.8	285.5	300.4
971.5	397	19.4	12.6	294.6	294.7	822.7	1769	11.6	8.1	286.0	301.2
968.0	427	19.0	12.6	294.2	294.9	819.6	1800	11.1	7.8	285.4	301.0
964.5	458	19.0	12.3	294.2	295.1	816.6	1830	11.0	7.6	285.3	301.1
961.0	488	18.6	12.4	293.8	295.0	810.4	1891	10.8	7.4	285.1	301.8
957.5	519	18.3	12.6	293.5	295.0	807.4	1922	10.6	7.3	284.9	301.9
954.0	549	18.2	12.6	293.4	295.2	804.3	1952	10.6	7.3	284.9	302.1
950.5	580	18.0	12.1	293.1	295.2	801.3	1983	10.6	7.3	284.9	302.4
947.0	610	17.7	11.8	292.8	295.2	798.3	2013	10.8	7.4	285.1	302.9
943.4	641	17.5	11.6	292.5	295.4	795.3	2044	10.6	7.6	284.9	303.0
936.7	702	17.1	11.4	292.1	295.6	792.2	2074	10.0	7.8	284.3	302.8
933.2	732	17.0	11.0	291.9	295.8	789.3	2105	10.3	4.9	284.1	303.4
929.8	763	16.7	11.2	291.7	295.8	787.8	2120	10.4	5.3	284.3	303.6
926.4	793	16.3	11.5	291.3	295.8	786.3	2135	10.3	5.5	284.2	303.6
923.0	824	16.0	11.4	291.0	295.7	783.6	2166	10.0	5.4	283.9	303.6
919.7	854	15.9	11.3	290.9	295.9	782.1	2181	9.9	6.1	284.0	303.6
916.2	885	15.7	11.0	290.6	296.2	780.7	2196	9.7	6.3	283.8	303.6

March 30, 1953. 1112 LST. Sounding in clear area near edge of cloudy area.
High cirrus present. Wind 110°, 5 m/sec. Location: 12 miles east-southeast of Anegada.

p (mb)	h (m)	T (°C)	w (gm/kgm)	T* (°A)	θ (°A)	p (mb)	h (m)	T (°C)	w (gm/kgm)	T* (°A)	θ (°A)
1012.9	34	25.2	16.6	301.2	297.1	928.1	795	19.2	13.1	294.5	298.8
1009.3	66	24.9	16.8	300.9	297.2	924.7	825	19.2	12.6	294.4	298.9
1005.6	96	24.4	17.0	300.4	297.2	921.3	857	18.9	12.5	294.1	299.0
1001.9	129	24.2	16.7	300.2	297.1	914.5	920	18.5	12.3	293.6	299.1
998.3	160	24.0	16.6	299.9	297.2	911.2	950	18.5	12.3	293.6	299.6
994.8	192	23.6	16.8	299.6	297.0	907.9	980	18.1	12.4	293.3	299.3
991.1	224	23.2	16.5	299.1	297.0	904.5	1010	17.8	12.5	293.0	299.3
987.5	256	23.0	16.4	298.9	297.2	901.2	1040	17.5	12.2	292.6	299.3
984.0	288	22.8	16.0	298.6	297.3	897.9	1072	17.3	12.3	292.4	299.5
980.4	320	22.5	16.1	298.4	297.4	894.5	1104	17.1	12.4	292.3	299.6
976.7	351	22.3	15.9	298.1	297.4	891.1	1136	17.0	12.2	292.1	300.1
973.3	382	21.9	16.0	297.7	297.3	887.9	1168	16.9	11.6	291.9	300.1
969.8	413	21.7	15.5	297.4	297.4	884.7	1200	16.7	11.5	291.7	300.3
966.3	444	21.5	15.1	297.2	297.4	881.4	1232	16.1	11.4	291.1	300.1
962.8	475	21.2	15.1	296.9	297.4	878.3	1260	16.1	11.5	291.1	300.4
955.8	540	20.7	15.0	296.4	297.7	871.6	1325	15.8	11.6	290.8	300.7
952.3	570	20.4	14.2	295.9	297.6	868.4	1355	15.3	11.8	290.4	300.5
948.8	600	20.1	14.4	295.6	297.6	865.1	1386	15.0	11.5	290.0	300.5
945.3	633	20.0	14.2	295.5	298.0	861.9	1417	15.0	11.4	290.0	300.8
941.9	666	19.8	13.9	295.2	298.1	858.8	1448	14.8	11.5	289.8	300.9
938.4	699	19.6	14.0	295.1	298.0	855.5	1479	14.6	11.4	289.6	301.0
935.0	732	19.3	13.4	294.7	298.2	852.3	1510	14.6	11.1	289.5	301.2
931.5	765	19.2	13.4	294.6	298.2	845.9	1561	14.4	10.8	289.3	301.7

April 1, 1953. 1045 LST. Sounding in clear area near cloudy area.
Some cirrus present. Wind 146°, 4 m/sec. Location: 10 miles east of Anegada.

p (mb)	h (m)	T (°C)	w (gm/kgm)	T* (°A)	θ (°A)	p (mb)	h (m)	T (°C)	w (gm/kgm)	T* (°A)	θ (°A)
1014.8	15	24.9	15.6	300.7	296.7	928.1	788	18.5	11.9	293.6	297.9
1012.9	30	24.6	15.4	300.4	296.6	924.7	819	18.4	12.1	293.5	298.1
1009.3	65	25.0	15.3	300.7	297.2	921.3	850	18.0	12.1	293.1	298.1
1005.6	97	24.3	15.4	300.1	297.0	918.0	880	17.8	12.1	292.9	298.2
1001.9	128	24.1	15.2	299.8	297.1	914.5	913	17.8	11.5	292.8	298.5
998.3	160	23.7	15.3	299.4	296.9	911.2	944	17.9	11.1	292.8	298.9
994.8	192	23.5	15.4	299.3	297.0	904.5	1004	17.4	10.9	292.3	299.0
991.1	224	23.2	15.5	299.0	297.1	901.2	1034	17.2	10.8	292.1	299.1
987.5	256	22.9	15.0	298.6	297.1	897.9	1064	17.1	10.6	292.0	299.4
984.0	288	22.7	15.5	298.5	297.2	894.5	1095	16.6	10.7	291.5	299.2
980.4	320	22.2	15.1	297.9	297.0	878.3	1255	16.0	8.4	290.5	300.2
976.9	350	21.9	14.2	297.4	297.0	874.9	1287	15.8	8.4	290.3	300.4
973.3	382	21.6	14.3	297.1	297.0	871.6	1319	15.7	8.5	290.2	300.4
962.8	475	20.6	13.0	295.9	297.1	868.4	1351	15.2	8.4	289.7	300.4
959.3	506	20.4	12.7	295.6	296.9	865.1	1383	15.1	7.9	289.5	300.6
955.8	537	20.2	12.7	295.4	297.2	861.9	1415	15.0	7.7	289.3	300.8
952.3	568	20.2	12.6	295.4	297.4	858.8	1444	15.0	7.5	289.3	301.1
948.8	599	19.7	12.7	294.9	297.3	855.5	1473	14.9	6.9	289.1	301.3
945.3	630	19.5	12.5	294.7	297.4	852.3	1500	14.7	6.8	288.9	301.3
938.4	695	19.1	12.7	294.3	297.8	849.2	1525	14.6	6.5	288.7	301.5
935.0	726	18.5	12.5	293.7	297.4	845.9	1550	14.6	6.3	288.7	302.0
931.5	757	18.6	11.9	293.7	297.6						

April 2, 1953. 1445 LST. Sounding in clear area north of small cloudy area. Some cirrus present.
Wind 120°, 4 m/sec. Location: 5 miles east of Anegada.

p (mb)	h (m)	T (°C)	w (gm/kgm)	T* (°A)	θ (°A)	p (mb)	h (m)	T (°C)	w (gm/kgm)	T* (°A)	θ (°A)
1011.2	35	25.3	14.9	301.0	297.2	860.2	1420	15.1	8.8	289.6	301.0
1007.6	62	25.2	14.3	300.9	297.3	857.1	1456	15.1	7.5	289.4	301.5
1003.9	95	24.9	14.7	300.5	297.7	853.8	1485	15.2	7.3	289.5	301.7
1000.2	130	24.4	14.6	300.0	297.4	850.6	1520	15.2	8.3	289.7	302.2
996.6	155	24.3	14.8	300.0	297.6	847.5	1553	14.9	8.6	289.4	302.2
989.4	218	23.5	14.6	299.1	297.4	844.2	1588	14.5	9.0	289.1	301.9
985.8	254	23.1	14.5	298.7	297.4	838.0	1650	14.2	9.3	288.8	302.5
982.3	290	22.9	14.7	298.5	297.4	834.8	1680	14.6	5.2	288.5	303.0
978.7	320	22.4	14.4	298.0	297.2	831.7	1713	14.7	4.9	288.6	303.5
975.2	350	22.1	14.5	297.7	297.3	828.6	1745	14.5	4.5	288.3	303.6
971.6	380	21.6	14.3	297.1	296.9	825.5	1780	14.2	3.9	287.9	303.6
968.1	418	21.4	14.3	296.9	297.1	822.4	1810	14.0	3.7	287.9	303.7
964.6	445	21.1	14.5	296.7	297.1	819.3	1840	13.8	3.6	287.4	303.8
961.1	480	20.9	14.2	296.4	297.3	813.2	1900	12.7	7.6	287.0	303.3
957.6	507	20.5	14.5	296.1	297.2	840.9	1622	14.1	9.8	288.9	301.9
954.1	544	20.4	14.3	295.9	297.5	838.0	1650	14.1	9.6	288.7	302.4
950.6	570	20.0	14.1	295.5	297.3	834.8	1680	14.2	8.9	288.7	302.8
943.6	632	19.9	12.6	295.1	298.0	831.7	1713	14.0	8.6	288.5	303.0
940.2	668	19.9	11.4	294.9	298.3	828.6	1745	13.8	8.4	288.3	303.0
936.7	700	19.8	11.0	294.7	298.7	825.5	1780	13.6	8.3	288.0	303.0
933.3	735	19.6	10.9	294.5	298.7	822.4	1810	13.5	7.8	287.9	303.2
929.8	760	19.3	10.7	294.2	298.7	818.3	1840	13.5	6.6	287.6	303.5
926.4	795	19.0	10.8	293.9	298.8	816.2	1870	13.5	6.0	287.5	303.9
923.0	825	18.9	10.2	293.7	298.7	813.2	1900	13.0	7.2	287.2	303.6
919.6	855	18.9	9.6	293.6	299.1	807.0	1968	12.7	7.4	287.0	303.9
916.3	890	18.9	9.4	293.6	299.6	804.0	2000	11.8	7.5	286.1	303.3
912.8	915	18.8	9.3	293.4	299.6	800.9	2033	11.9	6.4	286.0	303.7
909.5	955	18.8	9.4	293.5	299.9	797.9	2065	11.6	6.7	285.7	303.7
906.2	985	18.3	9.6	293.0	299.7	794.9	2098	11.6	6.6	285.7	304.0
902.8	1015	18 2	9.2	292.8	299.7	791.9	2130	11.5	5.6	285.5	304.3
899.5	1042	17.9	9.9	292.6	299.9	788.8	2162	11.5	5.8	285.5	304.5
896.2	1075	17.9	9.2	292.5	300.4	785.9	2194	11.2	5.6	285.2	304.7
892.8	1105	17.6	9.2	292.3	300.3	782.9	2226	11.2	5.0	285.1	305.0
889.4	1140	17.3	9.2	291.9	300.5	780.1	2258	11.0	4.4	284.8	305.1
886.2	1170	17.2	9.1	291.8	300.8	777.3	2290	11.0	3.9	284.8	305.4
883.0	1200	17.0	9.4	291.7	300.9	774.5	2318	10.7	4.0	284.6	305.3
879.7	1230	16.7	9.5	291.4	300.9	771.6	2339	10.5	3.9	284.4	305.4
876.6	1260	16.4	9.5	291.1	300.8	768.7	2360	10.3	4.3	284.2	305.5
873.2	1295	16.3	9.7	290.0	301.0	765.7	2388	10.3	3.7	283.9	306.0
869.9	1325	16.2	9.4	290.8	301.2	760.0	2437	9.7	3.5	283.3	306.0
866.7	1355	15.6	9.3	290.2	301.0	754.0	2483	9.2	3.7	282.8	306.0
863.4	1390	15.5	8.8	290.0	301.1						

April 4, 1953. 1150 LST. Sounding in clear area. No clouds except over islands.
Wind 140°, 6 m/sec. Location: 5 miles east of Anegada.

p (mb)	h (m)	T (°C)	w (gm/kgm)	T* (°A)	Θ (°A)	p (mb)	h (m)	T (°C)	w (gm/kgm)	T* (°A)	Θ (°A)
1014.4	23	26.2	15.0	301.9	298.0	904.8	1014	18.2	9.6	292.9	299.8
1009.6	65	25.4	14.6	301.0	297.6	898.2	1075	17.5	9.9	292.2	299.6
1005.9	100	25.0	14.4	300.6	297.6	894.8	1107	17.4	9.9	292.1	299.9
1002.2	130	24.6	14.1	300.1	297.5	891.4	1140	17.0	10.1	291.8	299.9
998.6	163	24.3	14.3	299.9	297.5	888.2	1170	16.8	9.9	291.5	300.1
995.1	195	24.1	14.3	299.7	297.6	885.0	1202	16.7	9.2	291.3	300.3
991.4	228	23.8	14.4	299.4	297.6	868.7	1360	15.2	9.1	289.8	300.2
987.8	259	23.4	14.6	299.0	297.7	865.4	1390	14.8	10.1	289.6	300.2
984.3	290	23.0	14.4	298.6	297.6	862.2	1423	14.6	10.2	289.4	300.4
980.7	322	22.7	14.2	298.2	297.5	859.1	1457	14.6	10.2	289.4	300.8
977.2	354	22.6	14.1	298.1	297.6	855.8	1490	14.6	8.1	289.0	301.0
973.6	385	22.2	14.3	297.7	297.7	852.6	1523	14.2	8.5	288.7	300.8
970.1	417	22.0	14.2	297.5	297.7	849.5	1556	14.1	8.3	288.6	301.1
966.6	449	21.9	14.0	297.4	297.8	846.2	1580	13.9	7.5	288.2	301.3
963.1	479	21.5	14.3	297.0	297.6	842.9	1615	13.9	7.3	288.2	301.4
959.6	511	21.2	14.1	296.7	297.6	840.0	1642	13.7	7.3	288.0	301.5
956.0	543	21.0	14.0	296.5	298.0	836.8	1674	13.6	7.3	287.9	301.8
952.6	575	20.8	13.8	296.1	297.8	827.5	1767	13.3	6.7	287.4	302.6
949.1	607	20.4	14.1	295.9	298.0	824.4	1799	13.4	5.5	287.4	302.9
945.6	639	20.0	14.1	295.5	298.0	821.3	1830	13.6	5.3	287.5	303.4
942.2	669	19.8	13.7	295.2	298.1	818.2	1860	13.6	5.7	287.6	303.6
938.7	699	19.8	13.8	295.2	298.3	815.2	1890	13.6	5.8	287.6	304.0
935.3	729	19.8	12.2	295.0	298.7	813.6	1907	13.6	6.4	287.7	304.2
931.8	759	19.7	11.6	294.7	298.7	812.1	1920	13.8	5.7	287.8	304.8
928.4	790	19.6	10.4	294.4	299.0	809.0	1945	14.0	4.9	287.9	304.9
925.0	822	19.4	10.2	294.2	299.2	806.0	1972	13.9	4.7	287.7	305.3
921.6	854	18.9	10.8	293.8	298.9	802.9	1999	13.6	4.8	287.4	305.2
918.3	886	18.9	10.1	293.7	299.2	801.4	2009	13.7	5.0	287.6	305.5
914.8	918	18.7	10.1	293.5	299.4	799.9	2021	13.7	4.8	287.5	305.9
911.5	950	18.8	9.6	293.5	299.6	796.9	2047	13.7	4.4	287.5	306.0
908.2	980	18.5	9.7	293.2	299.7						

April 5, 1953. 1300 LST. Sounding in clear area. No cumulus present except over islands.
Middle clouds 8/10. Wind 140°, 7.5 m/sec. Location: 10 miles east of Anegada.

p (mb)	h (m)	T (°C)	w (gm/kgm)	T* (°A)	Θ (°A)	p (mb)	h (m)	T (°C)	w (gm/kgm)	T* (°A)	Θ (°A)
999.8	130	23.8	14.6	299.4	296.9	822.0	1800	13.9	3.8	287.6	303.7
996.2	160	23.4	14.3	298.9	297.0	818.9	1830	13.9	3.9	287.6	304.0
992.7	190	23.4	13.4	298.8	297.2	815.8	1860	13.8	3.8	287.5	304.2
989.0	225	23.3	13.2	298.6	297.3	812.8	1890	13.7	3.8	287.4	304.3
985.4	257	23.1	13.6	298.5	297.5	806.6	1950	13.1	4.3	286.8	304.3
981.9	290	22.8	13.7	298.2	297.5	803.6	1990	12.7	4.0	286.4	304.3
978.3	320	22.4	13.4	297.8	297.6	800.5	2020	12.7	3.9	286.4	304.7
964.2	446	21.7	12.9	297.0	297.8	797.5	2060	12.5	4.0	286.2	304.7
960.7	476	21.6	11.7	296.7	297.9	794.5	2092	12.2	3.9	285.9	304.7
953.7	540	21.1	11.8	296.2	298.0	791.5	2124	11.9	4.1	285.6	304.9
950.2	570	20.6	11.8	295.7	297.8	788.4	2156	11.7	4.2	285.4	305.0
946.7	600	20.5	11.9	295.6	298.0	785.5	2188	11.7	4.0	285.3	305.1
943.2	630	19.9	12.6	295.1	297.9	782.5	2220	11.3	3.9	285.0	305.2
936.3	695	19.7	11.8	294.8	298.5	776.9	2284	10.4	4.7	284.2	305.0
932.9	730	19.5	11.7	294.5	298.4	774.1	2316	10.0	5.3	283.9	304.8
929.4	765	19.3	11.7	294.3	298.6	768.3	2380	9.4	5.8	283.4	304.7
926.0	795	19.0	11.8	294.1	298.8	765.3	2410	8.9	5.8	282.9	304.6
919.2	855	18.6	12.0	293.7	298.8	759.6	2470	9.0	6.1	283.0	305.1
915.9	885	18.4	11.9	293.5	299.0	756.6	2500	9.4	—	—	306.0
909.1	950	17.8	11.8	292.9	299.0	753.6	2530	9.3	—	—	306.2
905.8	980	17.6	11.7	292.6	299.0	750.6	2565	9.6	9.5	284.2	307.1
902.4	1010	17.5	11.9	292.6	299.3	744.9	2625	9.7	8.9	284.2	307.9
899.1	1040	17.1	11.6	292.1	299.2	742.1	2660	9.5	9.0	284.0	308.0
895.8	1070	16.8	11.6	291.8	299.3	736.5	2720	9.1	9.1	283.7	308.1
885.8	1170	16.1	11.3	291.1	299.6	733.7	2748	9.0	9.2	283.6	308.3
879.3	1240	15.6	10.3	290.4	299.8	730.9	2776	9.1	8.6	283.6	308.8
876.2	1270	15.3	10.5	290.1	299.9	728.1	2804	9.3	8.4	283.7	309.3
872.8	1292	15.2	10.0	290.0	300.0	722.6	2860	8.5	8.5	283.0	309.2
866.3	1356	14.4	9.6	289.1	300.0	717.1	2940	8.7	5.6	282.7	310.2
863.0	1388	14.7	8.9	289.1	300.4	714.4	2972	8.5	5.2	282.4	310.4
859.8	1430	14.7	7.7	289.0	300.7	708.9	3036	8.3	4.7	282.1	310.5
853.4	1490	14.5	7.1	288.7	301.2	706.2	3068	8.1	2.9	281.6	310.9
850.2	1520	14.6	6.5	288.7	301.6	703.5	3100	8.0	2.5	281.4	311.0
847.1	1550	14.6	5.7	288.6	301.8	700.8	3130	7.8	1.9	281.1	311.2
843.8	1580	14.5	5.6	288.5	302.1	698.0	3162	7.7	1.1	280.9	—
837.6	1640	13.8	5.5	287.7	301.9	689.9	3230	7.1	1.1	280.3	—
828.2	1740	13.9	5.1	287.8	303.2	687.1	3252	6.8	1.2	280.0	—
825.1	1770	13.9	4.1	287.6	303.4						

April 7, 1953. 0950 LST. Sounding in cloudy area.
Wind 96°, 5.5 m/sec. Location: 20 miles north of Anegada.

p (mb)	h (m)	T (°C)	w (gm/kgm)	T* (°A)	Θ (°A)	p (mb)	h (m)	T (°C)	w (gm/kgm)	T* (°A)	Θ (°A)
1013.1	12	24.9	15.2	300.6	296.8	919.6	853	18.7	10.6	293.5	298.9
1011.2	28	24.7	14.6	300.3	296.7	916.3	885	18.6	10.9	293.5	299.1
1007.6	66	24.9	14.6	300.5	297.1	912.8	915	18.1	11.2	293.1	298.9
1003.9	95	24.1	14.6	299.7	296.7	909.5	945	18.1	11.1	293.0	299.1
1000.2	130	24.0	14.4	299.6	297.0	906.2	978	17.6	11.5	292.6	299.2
996.6	156	23.5	14.4	299.1	296.7	902.8	1010	17.7	10.9	292.6	299.5
993.0	193	23.3	14.2	298.8	297.0	899.5	1040	17.8	10.7	292.7	299.9
989.4	229	23.1	14.1	298.6	297.0	896.2	1071	17.2	10.4	292.0	299.6
985.8	255	22.8	14.2	298.3	297.0	892.8	1100	17.0	10.3	291.8	299.7
982.3	290	22.4	14.3	297.9	297.1	886.2	1170	16.9	9.4	291.5	300.3
978.7	318	21.8	14.0	297.3	296.8	879.7	1230	16.6	9.3	291.2	300.8
975.2	353	21.8	14.1	297.3	297.1	876.6	1262	16.2	9.3	290.8	300.5
971.6	385	21.6	14.0	297.1	297.0	873.2	1292	16.0	8.9	290.5	300.6
968.1	418	21.2	14.1	296.7	297.1	869.9	1323	15.9	8.9	290.4	301.0
964.6	447	20.9	14.1	296.4	297.0	866.7	1355	15.7	8.2	290.1	300.9
961.1	478	20.6	13.9	296.0	297.1	863.4	1387	15.6	8.3	290.1	301.2
957.6	510	20.2	14.1	295.7	297.0	860.2	1420	15.6	7.8	290.0	301.5
954.1	541	20.3	13.6	295.7	297.3	857.1	1453	15.3	7.4	289.6	301.5
950.6	574	19.8	13.6	295.2	297.2	853.8	1479	15.3	6.5	289.4	301.8
947.1	601	19.7	13.2	295.0	297.3	850.6	1505	15.3	5.4	289.2	302.1
940.2	665	19.0	13.6	294.2	297.5	847.5	1531	15.3	4.4	289.1	302.4
936.7	698	19.2	12.4	294.4	297.6	844.2	1560	14.9	4.2	288.6	302.7
933.3	729	18.9	12.2	294.1	297.7	840.9	1590	14.6	4.1	288.3	302.6
929.8	760	18.7	11.8	293.8	297.8	831.7	1666	14.5	6.6	288.6	303.3
926.4	793	18.5	11.6	293.5	298.1	828.6	1696	14.4	6.6	288.5	304.4
923.0	823	18.7	10.8	293.6	298.5						

APPENDIX II

TABLE 3. STRUCTURE OF TRANSITION AND CLOUD LAYERS FOR SERIES H (1946) SOUNDINGS

	TRANSITION LAYER						CLOUD LAYER						
Date and Time (local)	Depth m	$\Delta\theta$ °C	$-\partial T/\partial z$ °C/100m	$-\partial T^*/\partial z$ °C/100m	$-\partial w/\partial z \cdot 10^8$ cm^{-1}	$\overline{rh}$ %	Depth m	$-T\partial/\partial z$ °C/100m	$-\partial T^*/\partial z$ °C/100m	$-\partial w/\partial z \cdot 10^8$ cm^{-1}	$\overline{rh}$ %	Height of Trade Inversion m	Remarks
April 10 1524 hrs. clear	216	1.2	0.37	0.58	12.3	87				Sounding ended too low			
April 12 1423 hrs. clear	320	1.9	0.48	0.57	10.5	71	1185	0.65	0.67	0.5	61	1885	
April 12 1505 hrs. cloudy	116	0.3 Layer	0.86 effectively	0.91 missing	2.0	88	Msg.	0.53	0.62	5.4	88	Msg.	Lapse rates only to 1500 m.
April 12 1534 hrs. clear	125	2.0	0.56	0.72	6.0	84	Msg.	0.64	0.73	4.6	81	Msg.	Lapse rates only to 1500 m.
April 13 1323 hrs. clear	275	1.9	0.51	0.67	12.0	79	1770	0.71	0.75	1.7	69	2440	Trade inversion located on radiosonde (San Juan)
April 13 1414 hrs. cloudy	110	1.2 Layer	0.73 effectively	1.0 missing	3.6	93				Sounding ended too low			
April 13 1454 hrs. clear	110	1.2	0.45	0.64	14.5	84				Sounding ended too low			
April 13 1533 hrs. clear	274	2.4	0.04	0.49	21	69				Sounding ended too low			
April 14 0008 hrs. clear	72	2.1	0.21	0.76	32	83				Sounding ended too low			
April 14 0615 hrs. clear	79	1.4	0.34	0.76	16	76	1870	0.66	0.74	2.1	79	2470	
April 14 0720 hrs. cloudy	98	1.1	0.76	0.92	14	81	1850	0.65	0.72	2.7	78	2530	
April 22 1854 hrs. clear	226	1.8	0.55	0.71	10.5	85	1191	0.65	0.71	3.8	78	1905	
April 23 0713 hrs. clear	177	2.1	0.73	0.85	5.2	93	Msg.	0.57	0.63	2.5	91	Msg.	Trough line Cunimb build-ups

TABLE 3. STRUCTURE OF TRANSITION AND CLOUD LAYERS FOR SERIES H (1946) SOUNDINGS — (*Continued*)

	TRANSITION LAYER						CLOUD LAYER						
Date and Time (local)	Depth m	$\Delta\Theta$ °C	$-\partial T/\partial z$ °C/100m	$-\partial T^*/\partial z$ °C/100m	$-\partial w/\partial z \cdot 10^8$ cm^{-1}	$\overline{rh}$ %	Depth m	$-\partial T/\partial z$ °C/100m	$-\partial T^*/z$ °C/100m	$-\partial w/\partial z \cdot 10^8$ cm^{-1}	$\overline{rh}$ %	Height of Trade Inversion m.	Remarks
April 23 1307 hrs. cloudy	116	0.2 Layer	0.78 effectively	1.0 missing	4.2	93	Msg.	0.64	0.69	3.9	90	Msg.	Portion 700–2000 m only
April 23 1353 hrs. clear	190	1.3	0.47	0.76	13.1	89	1860	0.57	0.62	2.6	82	2680	Disturbed day
April 25 1616 hrs. cloudy	275	0.2 Layer	0.97 effectively	1.15 missing	7.2	89	670	0.58	0.73	8.6	87	1310	
April 25 1646 hrs. clear	95	1.4	0.79	0.84	7.2	86	680	0.65	0.79	6.9	81	1265	
April 26 1319 hrs. cloudy	85	0.6	0.29	0.53	13.1	86	1000	0.70	0.82	4.6	73	1815	
April 26 1416 hrs. clear	183	0.4	0.74	0.93	14.7	82	1420	0.64	0.70	1.5	67	2215	
April 27 0923 hrs. cloudy	128	−0.4	1.32	1.6	16.8	92	912	0.64	0.75	6.7	58	1765	
April 27 1025 hrs. clear	314	1.7	0.47	0.74	17.5	70	1525	0.65	0.63	−1.15	75	2318	
April 27 1639 hrs. cloudy	177	0.4	0.59	0.85	11	82	Msg.	0.54	0.65	5.0	82	Msg.	Portion 700–2000 m
April 27 1728 hrs. clear	192	1.1	0.26	0.62	22	80	Msg.	0.53	0.62	1.3	56	Msg.	Portion 900–2100 m
April 28 0635 hrs. cloudy			Totally missing				Msg.	0.61	0.70	5.0	86	Msg.	Portion 900–2100 m
April 28 0725 hrs. clear	305	1.4	0.54	0.64	16.1	82	1590	0.66	0.68	2.6	77	2440 (radiosonde)	Portion 900–2100 m
Clear Av.	197	1.6	0.47	0.70	14.4	81		0.63	0.69	2.4	76		
Cloudy Av.	138*	0.4	0.79	0.995	9.0	88		0.61	0.71	5.2	79		
Total Av.	177	1.2	0.57	0.80	12.6	84	1328	0.62	0.70	3.5	77	2080	

* Effectively or totally missing in 5 cases out of 9. Average given for 8 cases out of 9